Lamin A/C and Emerin depletion impacts chromatin organization and dynamics in the interphase nucleus

Devika Ranade[†], Roopali Pradhan[†], Muhunden Jayakrishnan, Sushmitha Hegde and Kundan Sengupta[*]

Abstract

Background: Nuclear lamins are type V intermediate filament proteins that maintain nuclear structure and function. Furthermore, Emerin - an interactor of Lamin A/C, facilitates crosstalk between the cytoskeleton and the nucleus as it also interacts with actin and Nuclear Myosin 1 (NM1).

Results: Here we show that the depletion of Lamin A/C or Emerin, alters the localization of the nuclear motor protein - Nuclear Myosin 1 (NM1) that manifests as an increase in NM1 foci in the nucleus and are rescued to basal levels upon the combined knockdown of Lamin A/C and Emerin. Furthermore, Lamin A/C-Emerin co-depletion destabilizes cytoskeletal organization as it increases actin stress fibers. This further impinges on nuclear organization, as it enhances chromatin mobility more toward the nuclear interior in Lamin A/C-Emerin co-depleted cells. This enhanced chromatin mobility was restored to basal levels either upon inhibition of Nuclear Myosin 1 (NM1) activity or actin depolymerization. In addition, the combined loss of Lamin A/C and Emerin alters the otherwise highly conserved spatial positions of chromosome territories. Furthermore, knockdown of Lamin A/C or Lamin A/C-Emerin combined, deregulates expression levels of a candidate subset of genes. Amongst these genes, both KLK10 (Chr.19, Lamina Associated Domain (LAD+)) and MADH2 (Chr.18, LAD-) were significantly repressed, while BCL2L12 (Chr.19, LAD-) is de-repressed. These genes differentially reposition with respect to the nuclear envelope.

Conclusions: Taken together, these studies underscore a remarkable interplay between Lamin A/C and Emerin in modulating cytoskeletal organization of actin and NM1 that impinges on chromatin dynamics and function in the interphase nucleus.

Keywords: Nucleus, Chromosome territories, Lamin A/C, Emerin, Nuclear myosin 1, Actin

Background

Chromosomes are organized as Chromosomes Territories (CT) in the interphase nucleus. Gene rich chromosome territories are positioned near the nuclear interior, while gene poor chromosome territories are proximal to the nuclear periphery [1, 2]. Fluorescence microscopy and contact based chromatin maps such as Chromosome Conformation Capture (3C) and Hi-C further reiterate the non-random organization of the genome [1–4].

Lamins are type V intermediate filament proteins, enriched at the nuclear envelope that regulate nuclear structure-function relationships and are required for maintaining the non-random organization of chromosome territories [5]. Lamin A and Lamin C are encoded by the LMNA gene, while B type lamins (Lamin B1 and Lamin B2) are encoded by two different genes - LMNB1 and LMNB2 [6, 7]. Lamins A, C, B1 and B2 form separate but interacting microdomains in the nucleus [5, 8]. While B type lamins are expressed in all cells, Lamin A/C expression is lower in stem cells and increases as cells differentiate [9–12]. In addition to their localization and abundance at the nuclear envelope, a sub-fraction of both A and B type Lamins also exist in the nucleoplasm [13–20]. Furthermore, Lamins are also involved in

* Correspondence: kunsen@iiserpune.ac.in
[†]Devika Ranade and Roopali Pradhan contributed equally to this work.
Indian Institute of Science Education and Research (IISER)-Pune, Dr. Homi Bhabha Road, Biology, Room#B-216, 1st Floor, Main Building, Pashan, Pune, Maharashtra 411008, India

transcription, replication, DNA repair and senescence [21–24]. Lamins interact with chromatin either directly [25–28] or indirectly through chromatin binding proteins. B type lamins interact with Lamin B Receptor (LBR) and HP1α associated with heterochromatin [29], while A type lamins interact with proteins associated with both hetero and euchromatin namely LAP2α, Emerin and BANF1 [30–32]. A and B type lamins along with their interactors such as Emerin and LAP2β (Lamina associated polypeptide 2β) associate with chromatin at 'Lamina Associated Domains (LADs)' [33–35]. LADs are ~ 0.1–10 Mb stretches of chromatin bearing Lamina Associated Sequences (LASs), characterized by high density of repeat rich DNA and inactive histone marks H3K9me2/3 [33, 36, 37]. LADs bound by B type lamins are proximal to the nuclear envelope, while those bound by A type lamins exist both at the nuclear periphery and interior respectively [38, 39].

The functional dichotomy between the sub-interactomes of Lamins at the nuclear interior (Lamin A/C with LAP2α, BANF1) and nuclear periphery (Lamin A/C with Emerin, SUN1, SUN2, Nesprin-1α, Nesprin-2 and B-type Lamins with LBR, HP1α) is unclear [29–32, 40–45]. The contrasting organization of Lamin A at the nuclear envelope as a meshwork, and the nuclear interior as foci, short fibrous structures or unstructured nucleoplasmic 'veil' suggests differential associations of Lamin A with its interactors, resulting in distinct downstream effects on chromatin organization and function [8, 16, 20, 46–51]. Interestingly, in stem cells depleted of all Lamins, LAD organization is maintained by Emerin - a member of the LEM-D protein family, that interacts with Lamin A/C at the nuclear envelope [52].

Mutations in Lamin A/C and Emerin are associated with muscular dystrophies, suggestive of cell type specific co-regulation in Lamin A/C and Emerin function [53]. Lamin A mutations associated with cardiomyopathy (E161K) and progeria (G608G) show aberrant chromosome positions and gene expression profiles [54–57]. Additionally, patient-derived fibroblasts with laminopathy mutations (R89L, E358K, R482L in LMNA) and X-EDMD fibroblasts (ED5364, with mutations in EMD) reposition CT13 and CT18 (gene poor) toward the nuclear interior [58]. Emerin is localized at the interface of the cytoplasm and the nucleus, and functions as a mechanosensitive protein which regulates the response of the genome to external mechanical stimuli [59–61]. Furthermore, Emerin and Lamin A/C bind to actin and nuclear myosin 1 [62, 63]. Nuclear myosin 1 (NM1) is required for chromatin remodeling during transcription by RNA Polymerase I, II and III and functions in actin assisted long range chromatin movements [64–67]. A complex involving Lamin A/C-Emerin-NM1 along with actin, modulates chromatin dynamics [62, 68–72]. Emerin stabilizes the growing ends

of F-actin, while Lamin A/C binds to and regulates the levels of G-actin in the nucleus [62, 63, 73–75].

Here we show that the loss of Lamin A/C or Emerin alters cytoskeletal organization with an increase in nuclear NM1 foci and actin stress fiber aggregates. Loss of Lamin A/C and Emerin, further alters chromosome territory positions and enhances chromatin mobility, which was rescued to basal levels upon NM1 inhibition or actin depolymerization. Remarkably, Lamin A/C and Emerin alters expression levels of genes, which further show differential association with the nuclear envelope. In summary, these results underscore a remarkable role for Lamin A/C and Emerin as modulators of cytoskeletal and chromatin organization in the interphase nucleus.

Results

Lamin A/C or Emerin knockdown increases nuclear myosin 1 (NM1) foci in the nucleus

Emerin is localized in the cytoplasm and at the nuclear envelope of cells [76, 77]. Lamin A/C and Emerin are part of a nuclear sub-complex, that partner with Nuclear Myosin 1 (NM1) and actin [62, 63, 73]. NM1 and actin independently modulate chromatin dynamics and long range chromatin movements [66, 67, 78]. Furthermore, NM1 associates with chromatin, while G-actin assists chromatin remodeling in gene rich regions, predominantly toward the nuclear interior [65, 68, 79, 80]. We sought to investigate the impact of single and combined knockdowns (Kd) of Lamin A/C and its interacting partner – Emerin, on the subcellular localization of NM1 and actin in DLD-1 cells. Both single and combined knockdowns, depleted Lamin A/C and Emerin to ~ 70%, as ascertained independently by immunoblotting and immunofluorescence assays respectively (Fig. 1a-c).

We examined the subcellular localization of NM1 upon single and co-depletion of Lamin A/C and Emerin by immunofluorescence staining (Fig. 2a-b). NM1 is typically localized at the plasma membrane as a dense fibrous network and marginally in the nucleoplasm as punctate foci [81] (Fig. 2a-b, untreated, siLacZ). As reported previously, Lamin A/C knockdown results in an extranuclear aggregation of Emerin (Additional file 1a-b) [82]. Interestingly, Lamin A/C Kd alone, also showed a significant increase in NM1 aggregates outside the nucleus (Fig. 2b-c). Additionally, the number of intranuclear NM1 foci showed a significant increase upon both the single depletions of Lamin A/C and Emerin (Fig. 2d, Additional file 1c). Remarkably, NM1 localization was unaltered in the Lamin A/C and Emerin co-depleted cells (Fig. 2c-d, Additional file 1c). Immunoblotting did not show a significant change in the total levels of NM1 in either single or co-depletions of Lamin A/C and Emerin (Additional file
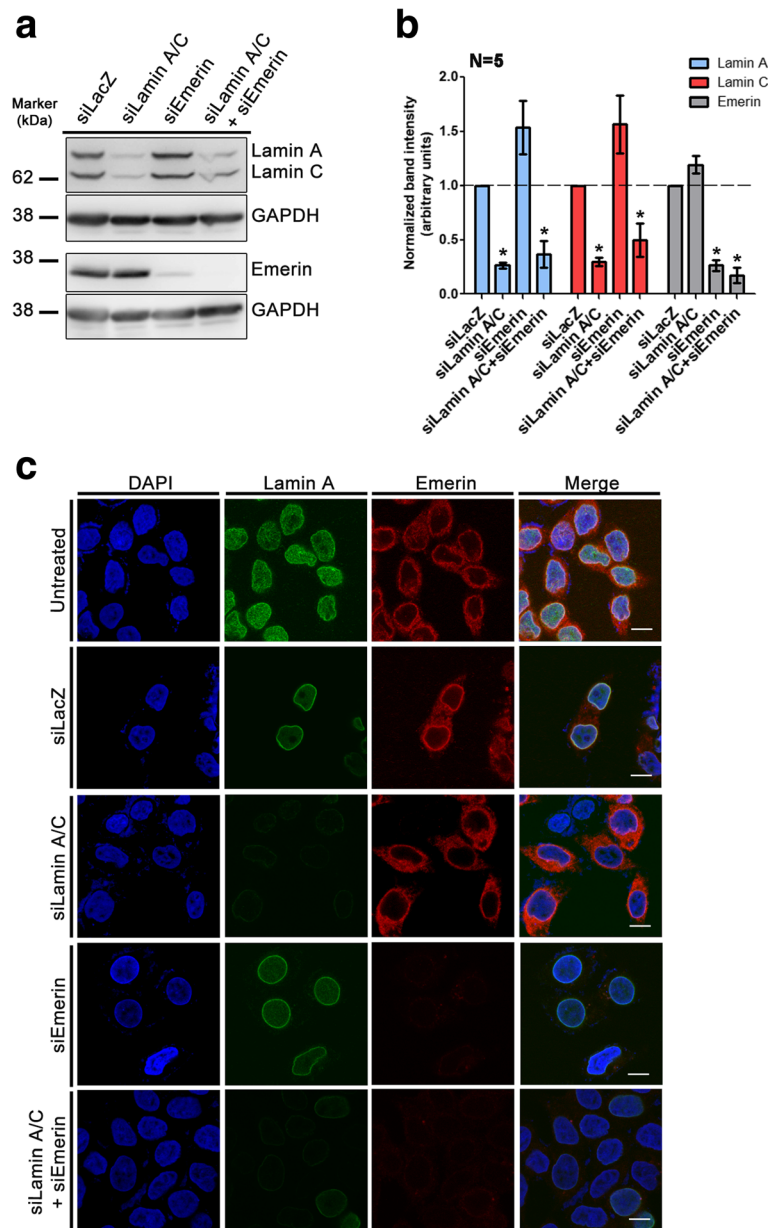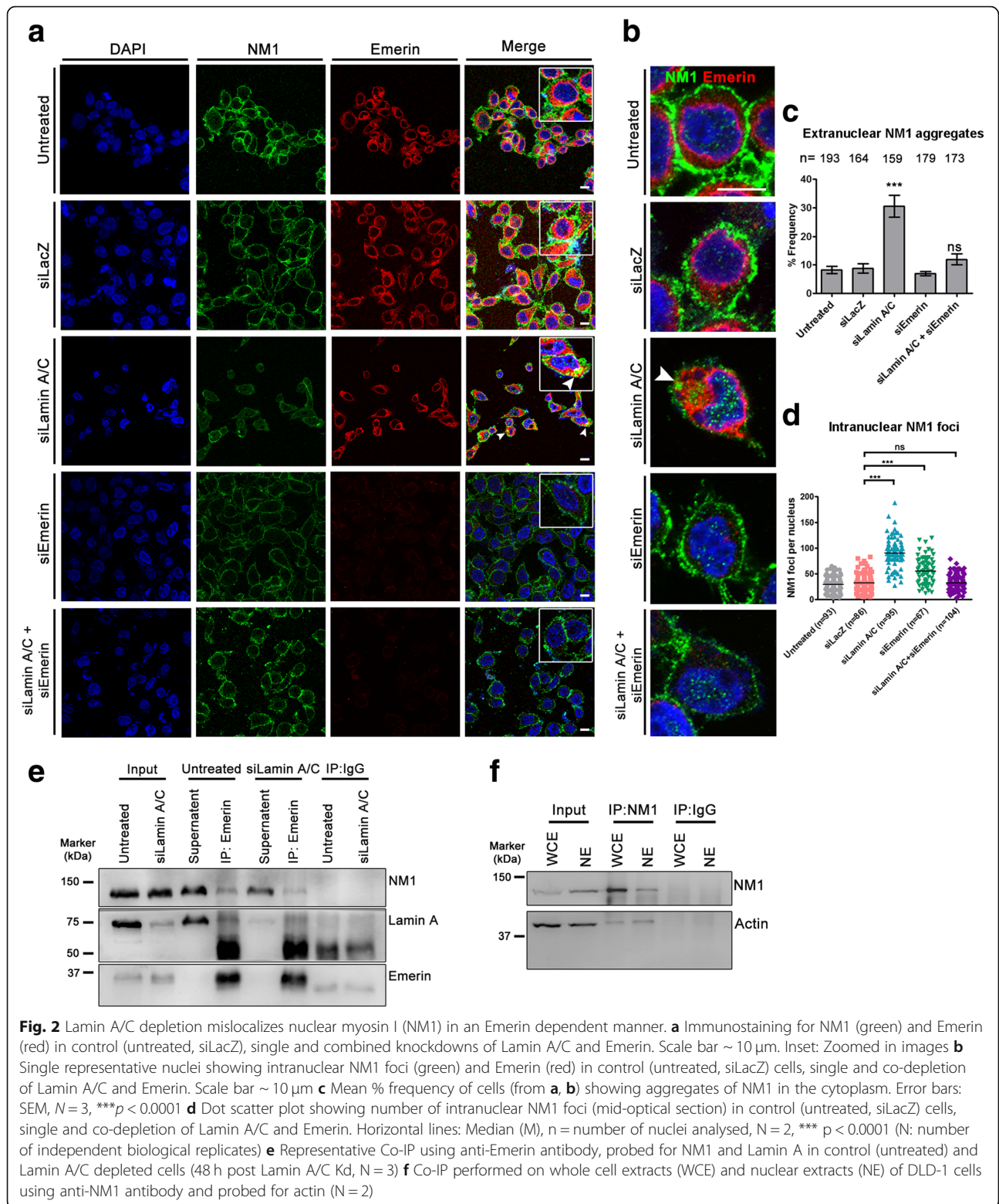
Fig. 1 Lamin A/C and Emerin knockdowns in DLD-1 cells. **a** Representative western blot showing single or combined knockdowns of Lamin A/C, Emerin in DLD-1 cells. Control: non-targeting siRNA (siLacZ), Loading control: GAPDH. **b** Densitometric quantification of band intensities for Lamins A, C and Emerin ($N = 5$ independent biological replicates, *$p < 0.05$). This shows ~ 75–80% knockdown of Lamin A/C and Emerin in both single and co-depletions respectively **c** Immunostaining of Lamin A (green) and Emerin (red) in single and co-depleted DLD-1 cells. Scale bar ~ 10 μm, ($N = 2$, data compiled from two independent biological replicates (N))

2a-b). Taken together, this suggests that Lamin A/C and Emerin modulate the nuclear localization of NM1.

Consistent with previous studies, co-immunoprecipitation assays showed that Lamin A/C interacts with Emerin and Emerin is a known interactor of NM1 (Fig. 2e) [30, 62]. Furthermore, Lamin A/C knockdown, reduces the association between Emerin and NM1, suggesting that Lamin A/C stabilizes Emerin-NM1 interaction (Fig. 2e, Additional file 2c-d). Independent co-immunoprecipitation assays also

revealed an association between NM1 and actin in the nucleus (Fig. 2f) [83]. In summary, these results implicate Lamin A/C as a modulator of NM1 localization in cells, as it regulates the stability of Emerin-NM1 interactions.

Lamin A/C-Emerin loss enhances actin stress fibers in cells

Lamin A/C and Emerin independently modulate actin polymerization in cells [62, 63, 73]. The arrangement of

Fig. 2 Lamin A/C depletion mislocalizes nuclear myosin I (NM1) in an Emerin dependent manner. **a** Immunostaining for NM1 (green) and Emerin (red) in control (untreated, siLacZ), single and combined knockdowns of Lamin A/C and Emerin. Scale bar ~ 10 μm. Inset: Zoomed in images **b** Single representative nuclei showing intranuclear NM1 foci (green) and Emerin (red) in control (untreated, siLacZ) cells, single and co-depletion of Lamin A/C and Emerin. Scale bar ~ 10 μm **c** Mean % frequency of cells (from **a**, **b**) showing aggregates of NM1 in the cytoplasm. Error bars: SEM, $N = 3$, ***$p < 0.0001$ **d** Dot scatter plot showing number of intranuclear NM1 foci (mid-optical section) in control (untreated, siLacZ) cells, single and co-depletion of Lamin A/C and Emerin. Horizontal lines: Median (M), n = number of nuclei analysed, N = 2, *** $p < 0.0001$ (N: number of independent biological replicates) **e** Representative Co-IP using anti-Emerin antibody, probed for NM1 and Lamin A in control (untreated) and Lamin A/C depleted cells (48 h post Lamin A/C Kd, N = 3) **f** Co-IP performed on whole cell extracts (WCE) and nuclear extracts (NE) of DLD-1 cells using anti-NM1 antibody and probed for actin (N = 2)

F-actin filaments impacts cell morphology, contractility and cell mechanics [84]. Cells on micropatterned substrates show increased actin polymerization and decreased diffusion of labelled H2B, suggesting an impact of altered actin organization on the nucleus and chromatin dynamics [69].

We stained untreated DLD-1 cells with Phalloidin, which shows a distinct cobblestone morphology characteristic of

epithelial cells, with relatively fewer stress fibers (Fig. 3a). Lamin A/C depletion alone did not appreciably alter actin stress fibers (Fig. 3a-b). In contrast, Emerin knockdown showed a significant increase in cells with actin stress fibers (~ 23%, arrowheads, Fig. 3a-b). Combined knockdown of Lamin A/C and Emerin also increased actin stress fibers in cells (~ 35%, arrowheads, Fig. 3a-b). Interestingly, we observed a decrease in actin levels in the nucleus as compared to the cytoplasm, upon immunoblotting nuclear and cytoplasmic extracts prepared from Emerin and Lamin A/C-Emerin co-depleted cells (Fig. 3c-e, Additional file 3c-d). Taken together, Lamin A/C and Emerin modulate subcellular distribution and organization of actin in cells.

Lamin A/C and Emerin co-depletion mislocalizes chromosome territory positions

Lamin A/C interacts with Emerin at the inner nuclear membrane [30]. Lamin A/C and Emerin regulate nuclear shape, mechanosignaling and chromatin organization via their common interactor - Barrier to Autointegration Factor (BAF) [30, 75, 85]. We previously showed that loss of Lamin A/C alone, does not alter the spatial positions of chromosome 18 and 19 territories in diploid DLD-1 cells [86].

We asked if the co-depletion of Lamin A/C and Emerin perturbs chromosome territory positions in DLD-1 cells (Additional file 3a). We examined positions of chromosome 18 and 19 territories since CT18 (Gene Density ~ 12.35 genes/Mbp, Size: 80 Mbp) and CT19 (Gene Density ~ 42.05 genes/Mbp, Size: 59 Mbp) are of comparable DNA content but strikingly contrasting gene densities (Fig. 4a) [1, 87, 88]. Lamin A/C or Emerin knockdowns did not alter the conserved spatial positions of either CT18 (peripheral) or CT19 (internal) in the nucleus (Fig. 4b-c, Table 1). Remarkably, co-depletion of Lamin A/C and Emerin significantly repositioned gene rich CT19 away from the nuclear interior (Median (M) = 59.57% R.D, Control − siLacZ: M = 53.35% R.D) (Fig. 4c, Table 1). However, the otherwise peripheral nuclear location of CT18 was unaltered upon the co-depletion of Lamin A/C and Emerin (M = 75.46% R.D, Control - siLacZ: M = 74.85% R.D) (Fig. 4b, Table 1), despite the spatial proximity of gene poor CT18 to the nuclear envelope.

We next determined the positions of another pair of chromosome territories i.e. gene rich CT17 (Gene Density ~ 29.3 genes/Mbp) and gene poor CT7 (Gene Density ~ 17.45 genes/Mbp) (Fig. 5a). Gene rich CT17 succeeds CT19 in gene density. The gene rich CT17 shifted more toward the nuclear interior upon Lamin A/C Kd (M = 53.42% R.D, Control - Untreated: M = 61.43% R.D) and in Lamin A/C-Emerin co-depleted cells (M = 50.27% R.D) (Fig. 5a-b, Table 2). However, similar to gene poor CT18, the positions of gene poor CT7 (peripheral),

remained unaltered in either single or combined knockdowns of Lamin A/C and Emerin (Fig. 5a, c, Table 2). Consistent with previous findings, Lamin A/C knockdown also affects the topology of chromosome territories (Additional file 4a-j) [56]. In summary, Lamin A/C and Emerin play a combined role in maintaining the conserved positions of chromosome territories present away from the nuclear envelope in the interphase nucleus.

Lamin A/C and Emerin co-depletion enhances chromatin mobility

Since the co-depletion of Lamin A/C and Emerin alters chromosome territory positions (Figs. 4 and 5), we asked if Lamin A/C or Emerin depletion impacts chromatin dynamics. We performed Fluorescence Recovery After Photobleaching (FRAP) of fluorescently labelled Histone 2A (H2A) in living cells as a readout of chromatin dynamics [89] (Fig. 6). We simultaneously quantified recovery profiles of fluorescently tagged H2A (H2A-mCherry) at the nuclear interior and periphery, in order to sample chromatin dynamics at diverse regions of the nucleus (Fig. 6a, Table 3). Interestingly, mobile fractions of H2A-mCherry showed a significant increase at the nuclear interior in Lamin A/C-Emerin co-depleted cells (Mobile Fraction - M.F ~ 31%, Control - siLacZ: M.F ~ 16%) (Fig. 6b, d). In contrast, chromatin mobility at the nuclear interior or periphery was largely unaltered in single knockdowns of either Lamin A/C or Emerin (Fig. 6b-d). Taken together, these results suggest that Lamin A/C and Emerin co-depletion increases chromatin dynamics in the interphase nucleus.

Rescue of chromatin mobility upon actin depolymerization and NM1 inhibition in Lamin A/C-Emerin co-depleted cells

The Lamin A/C-Emerin axis plays a crucial role in perceiving and relaying external mechanical signals into the nucleus and chromatin [59, 61, 85, 90–92]. Since we observed an impact of Lamin A/C-Emerin co-depletion on the subcellular distribution and organization of actin, we asked if destabilizing actin stress fibers impinges on chromatin mobility? We examined mobility of H2A-mCherry in Lamin A/C-Emerin co-depleted cells treated with Latrunculin A (Fig. 7a, Additional file 5a). Consistent with the previous experiment, combined knockdown of Lamin A/C and Emerin showed a significant increase in H2A-mCherry mobility toward the nuclear interior (siLamin A/C + siEmerin+DMSO: M.F ~ 25%, Control - siLacZ+DMSO: M.F ~ 14%) (Fig. 6b, 7b, Table 4). Remarkably, this enhanced mobility at the nuclear interior was restored to basal levels in Lamin A/C-Emerin co-depleted cells treated with Latrunculin A (M.F ~ 13%) (Fig. 7b, Table 4). H2A-mCherry mobility at the nuclear periphery was largely unaffected in Lamin A/
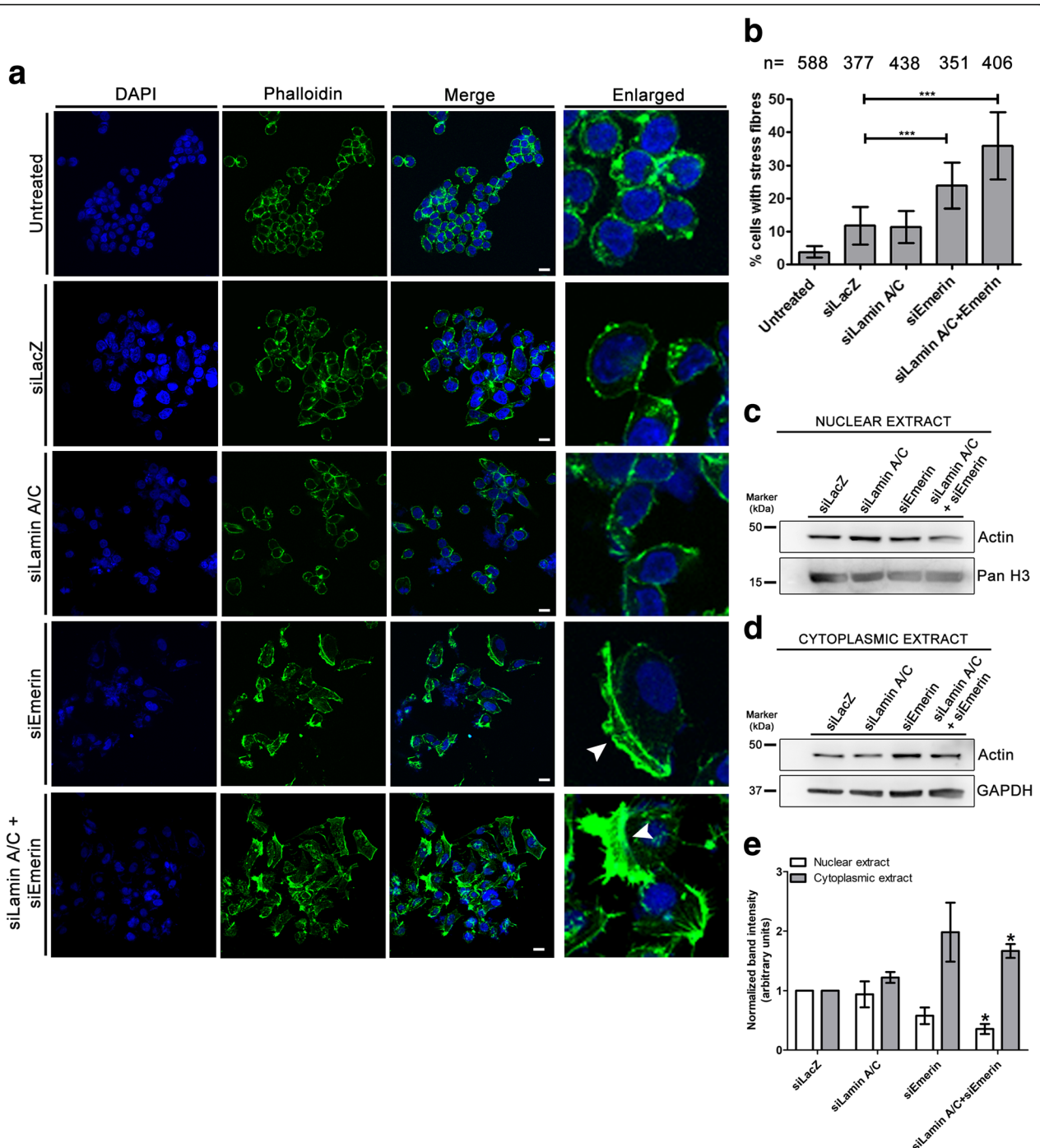
Fig. 3 Increase in actin stress fiber aggregates upon Lamin A/C-Emerin co-depletion. **a** Phalloidin staining (green) in control (untreated and siLacZ) cells, and upon single and co-depletion of Lamin A/C and Emerin. Scale bar ~ 10 μm. Enlarged: Zoomed in images. **b** % of cells with actin aggregates (from a), n = number of cells analysed, Error bars: SEM, N = 3, ***p < 0.0001 (N: number of independent biological replicates). **c** Representative western blot showing Actin levels in nuclear extracts of DLD-1 cells with single and combined depletion of Lamin A/C-Emerin **d** Representative western blot showing Actin levels in cytoplasmic extract of DLD-1 cells upon single and combined depletion of Lamin A/C-Emerin **e** Densitometric quantification of band intensity for Actin levels in nuclear and cytoplasmic extracts from cells with single and combined depletion of Lamin A/C-Emerin. Error bar: SEM, data compiled from N = 3 independent biological replicates, *p < 0.05
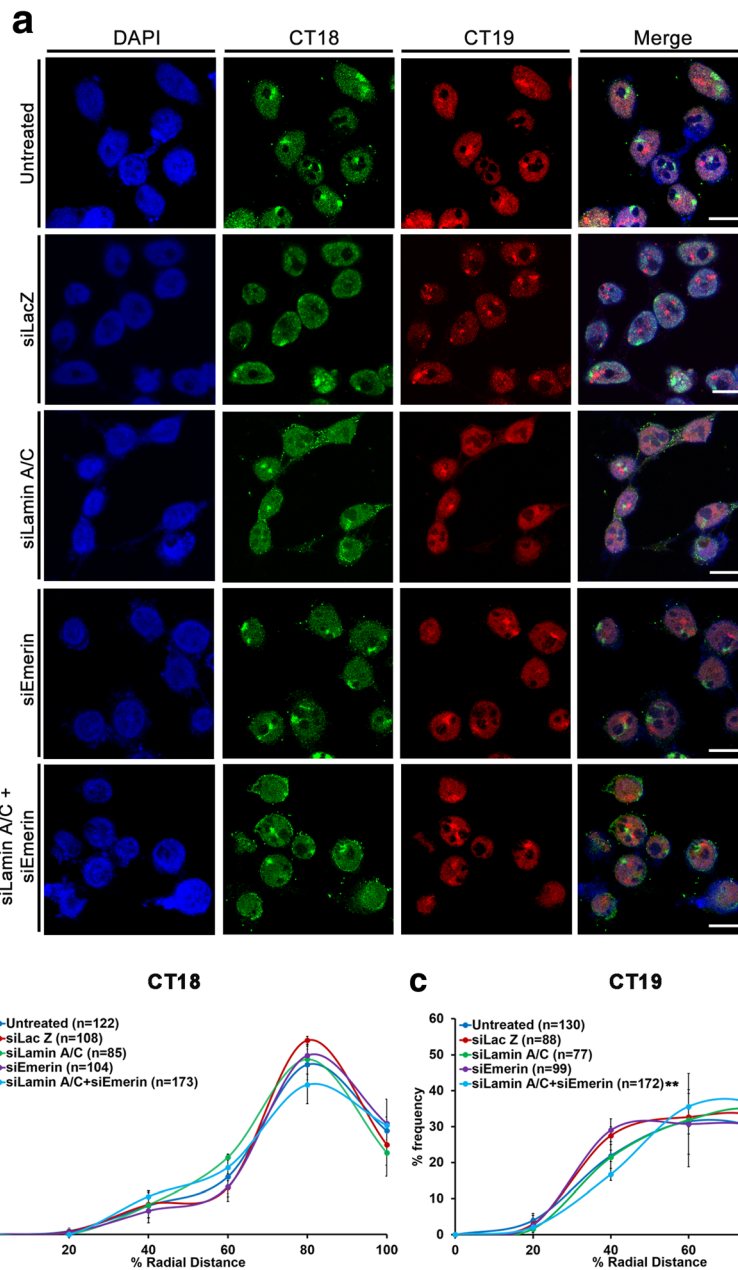
Fig. 4 Lamin A/C-Emerin co-depletion mislocalizes chromosome 19 territories. **a** Representative 3D-FISH images for CT18 (green) and CT19 (red) in control (untreated and siLacZ) cells, and single and co-depletion of Lamin A/C and Emerin. Scale bar ~ 10 μm. **b-c** Radial Distance (% R.D) distribution profiles for (**b**) CT18 and (**c**) CT19 in control (untreated and siLacZ) cells, and single and co-depletion of Lamin A/C and Emerin (X-axis: 0%: nuclear centre, 100%: nuclear periphery). Error bar: SEM, ** *p* < 0.01, n = number of CTs analysed, data compiled from N = 3 (N: number of independent biological replicates)

C-Emerin co-depleted cells in the presence or absence of Latrunculin A (Lat A) treatment (Fig. 7b, Table 4). Chromatin mobility was also unaffected upon Lat A treatment alone, either at the nuclear interior or periphery respectively (Additional file 5b-c). In summary, depolymerization of actin in Lamin A/C-Emerin co-depleted cells restores chromatin mobility to basal levels, comparable to control cells (siLacZ).

We next asked if inhibiting NM1 activity impacts chromatin mobility in the interphase nucleus. We quantified the mobile fractions of H2A-mCherry in Lamin A/C-Emerin co-depleted cells upon inhibition of NM1 using BDM (Fig. 7c, Table 5). Histone mobility was significantly enhanced upon Lamin A/C-Emerin co-depletion as observed previously (siLamin A/C + siEmerin+NFW: M.F ~ 30%, Control - siLacZ+NFW: M.F ~ 21%), and was restored

Table 1 Median % Radial Distance of CT18 and CT19 upon co-depletion of Lamin A/C and Emerin

Chromosome/Gene Density	Experiment	%Radial Distance (R.D)
CT18 (~ 12.35 genes/Mbp)	Untreated	72.52
	siLacZ	74.85
	siLamin A/C	71.17
	siEmerin	75.06
	siLamin A/C + siEmerin	75.46
CT19 (~ 42.05 genes/Mbp)	Untreated	53.52
	siLacZ	53.35
	siLamin A/C	51.65
	siEmerin	50.72
	siLamin A/C + siEmerin	59.57[a] ($p = 0.0091$)

[a]: statistically significant

to basal levels in Lamin A/C-Emerin co-depleted cells treated with BDM – an inhibitor of NM1 activity (M.F ~ 22%) (Fig. 7d, Table 5). H2A-mCherry mobility at the nuclear periphery was largely unaffected in Lamin A/C-Emerin co-depleted cells upon BDM treatment (Fig. 7d, Table 5). Taken together, these results underscore a combined role of Lamin A/C and Emerin in the regulation of actin organization and NM1 activity, which further impinges on chromatin dynamics in the nucleus.

Spatial positions of gene loci are altered upon Lamin A/C and Emerin depletion

Lamin A/C and Emerin regulate gene expression either directly or indirectly via other transcription factors [62, 93–102]. To examine the functional attributes of Lamin A/C and Emerin, we determined the expression levels of candidate genes (from human chromosomes 18 and 19), and their spatial localization in the interphase nucleus upon single and combined knockdowns of Lamin A/C and Emerin (Fig. 8a). Of the genes tested for expression changes, KLK10, BCL2L12 (both Chr. 19) and MADH2 (Chr. 18) showed transcriptional deregulation in both the single and co-depletions of Lamin A/C and Emerin (Fig. 8a). Interestingly, while KLK10 is within a Lamina Associated Domain (LAD), MADH2 is present between two neighboring LADs and BCL2L12 does not show LAD association or proximity (LAD-) (Fig. 8b, Additional files 6 a-h and 7a). We performed immuno-FISH assays to visualize the spatial localization of KLK10, BCL2L12 and MADH2 genes in the interphase nucleus, with reference to Lamin B1 staining as a marker of the nuclear envelope, as B-type lamins are unaffected upon Lamin A/C and Emerin knockdowns (Fig. 8c, Additional files 3 b and 7b). Measurement of the shortest distance from the nuclear envelope (Lamin B1 staining) revealed that KLK10 (LAD+), which was downregulated in both single and co-depletions of Lamin A/C

and Emerin, was re-positioned closer to the nuclear envelope in single Lamin A/C and Emerin knockdowns (Fig. 8a, c-d). However, its location was unaffected upon Lamin A/C-Emerin co-depletion (Fig. 8d). In contrast, MADH2 (between two neighboring LADs), is downregulated in single Lamin A/C Kd, Lamin A/C-Emerin co-depletion and upregulated in single Emerin Kd (Fig. 8a). MADH2 gene loci were re-positioned away from the nuclear envelope upon both single and co-depletions of Lamin A/C and Emerin respectively (Fig. 8e). Additionally, BCL2L12 (LAD-) showed a significant movement away from the nuclear envelope, consistent with its upregulation upon single and co-depletions of Lamin A/C and Emerin (Fig. 8f). Taken together, these studies suggest that Lamin A/C and Emerin modulate gene expression levels as well as the spatial positions of gene loci in the interphase nucleus. Consistent with the differential localization and organization of Lamin A/C at the nuclear envelope and in the nucleoplasm, it is likely that different and potentially specific sub-interactomes of lamins differentially modulate chromosome territory positions and chromatin dynamics at the nuclear interior and the nuclear periphery. The Lamin A/C-Emerin-Actin-NM1 network is therefore a key axis required for the maintenance of genome organization and function in the nucleus.

Discussion

The mechanisms that maintain chromosome position and function in the nucleus are largely unclear. Heterochromatin and gene poor chromosome territories are enriched in Lamina Associated Domains (LADs) and are localized toward the nuclear envelope [33, 39]. It is noteworthy that while B type lamins are largely associated with heterochromatin, Lamin A/C associates with both heterochromatin and euchromatin respectively [33, 103–105]. Here we show that the loss of Lamin A/C and Emerin significantly impacts subcellular localization of actin and NM1, which further impinges on chromatin organization (Figs. 2 and 3). Lamin A/C and Emerin regulate nuclear architecture via these interactors since actin depolymerization or NM1 inhibition restores enhanced chromatin dynamics to basal levels (Figs. 6 and 7).

Lamin A/C and Emerin knockdown enhances chromatin dynamics

Lamin A/C predominantly exists as coiled-coil filaments beneath the inner nuclear membrane [106] and as a phosphorylated nucleoplasmic sub-population [107]. Emerin is localized in the cytoplasm and at the inner nuclear membrane, where it interacts with Lamin A/C [30]. Unlike Lamin A/C, Emerin does not exist as a freely diffusing nucleoplasmic sub-pool. Lamin A/C and Emerin form independent and interdependent interactomes in the nucleus
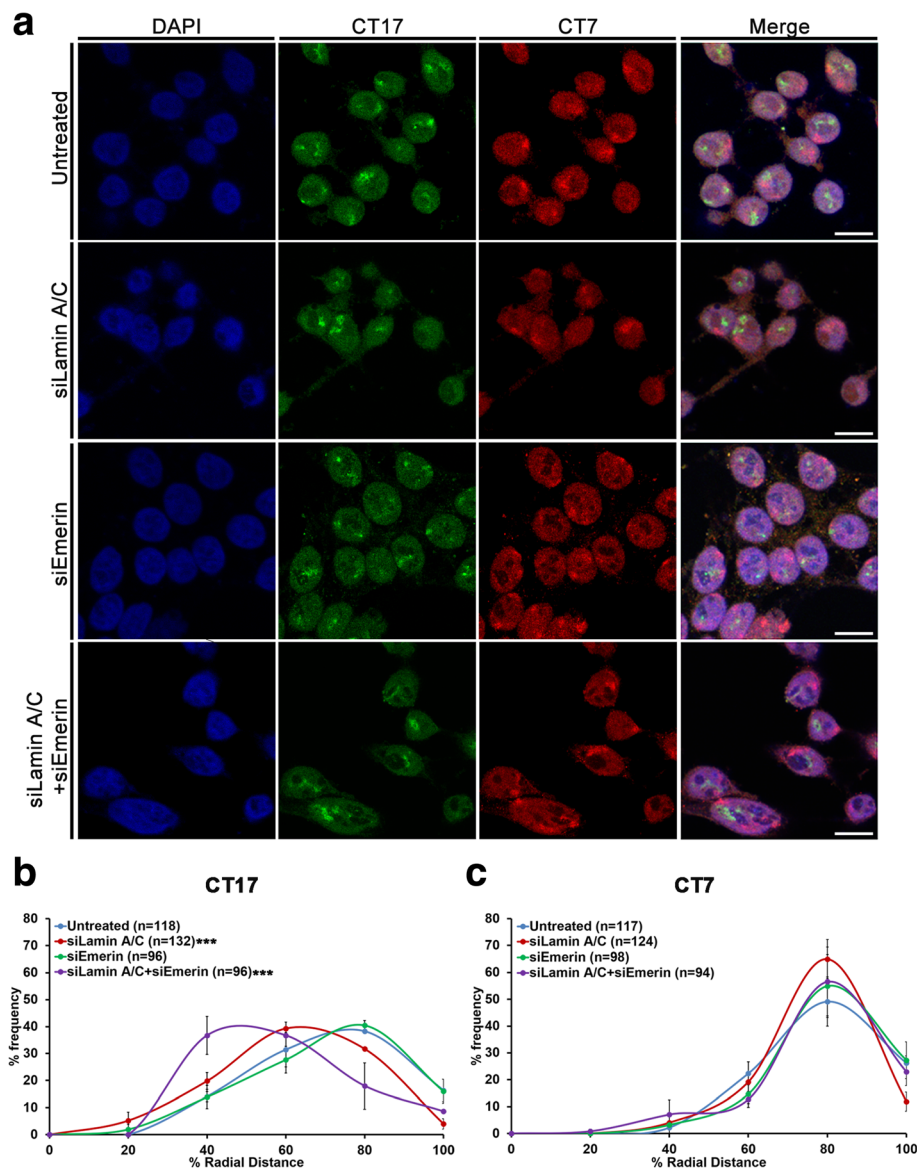
Fig. 5 Lamin A/C-Emerin co-depletion mislocalizes chromosome 17 territories. **a** Representative 3D-FISH images for CT7 (red) and CT17 (green) in control (untreated) cells, and single and co-depletion of Lamin A/C and Emerin. Scale bar ~ 10 μm. **b-c** Radial Distance (% R.D) distribution profiles for (**b**) CT17 and (**c**) CT7 in control (untreated) cells, and single and co-depletion of Lamin A/C and Emerin (X-axis: 0%: nuclear centre, 100%: nuclear periphery). Error bar: SEM, *** $p < 0.001$, n = number of CTs analysed, compiled data from N = 2 (N: number of independent biological replicates)

[108]. The nucleoplasmic veil of Lamin A/C modulates chromatin organization at the nuclear interior, potentially via direct or indirect interactions with BANF1 and LEM-D proteins [109]. Lamin A/C in the nuclear interior constrains the mobility of an artificially integrated LacO gene locus, further suggesting a role for Lamin A/C in modulating chromatin dynamics [110]. An increase in Lamin A/C expression in differentiating stem cells correlates with restrained chromatin dynamics in the nucleus [11]. We speculate that the combined loss of Lamin A/C and Emerin destabilizes its interactors at the nuclear interior and envelope respectively. Chromatin at the nuclear

periphery is associated with both A and B type Lamins, Emerin, Lamin B Receptor (LBR) and Lamina Associated Polypeptide 2β (LAP2β) among others [105, 111–113]. While euchromatin is associated with a nucleoplasmic sub-pool of Lamin A/C and interactors such as LAP2α [33, 103]. Notably, the localization of B type lamins was unaffected in Lamin A/C-Emerin co-depleted cells, highlighting a key role for Lamin A/C and Emerin in regulating chromatin dynamics (Additional file 3b). We surmise that Lamin A/C and Emerin co-depletion, potentially destabilizes its interactors at the nuclear interior, that therefore manifests as enhanced chromatin mobility at the
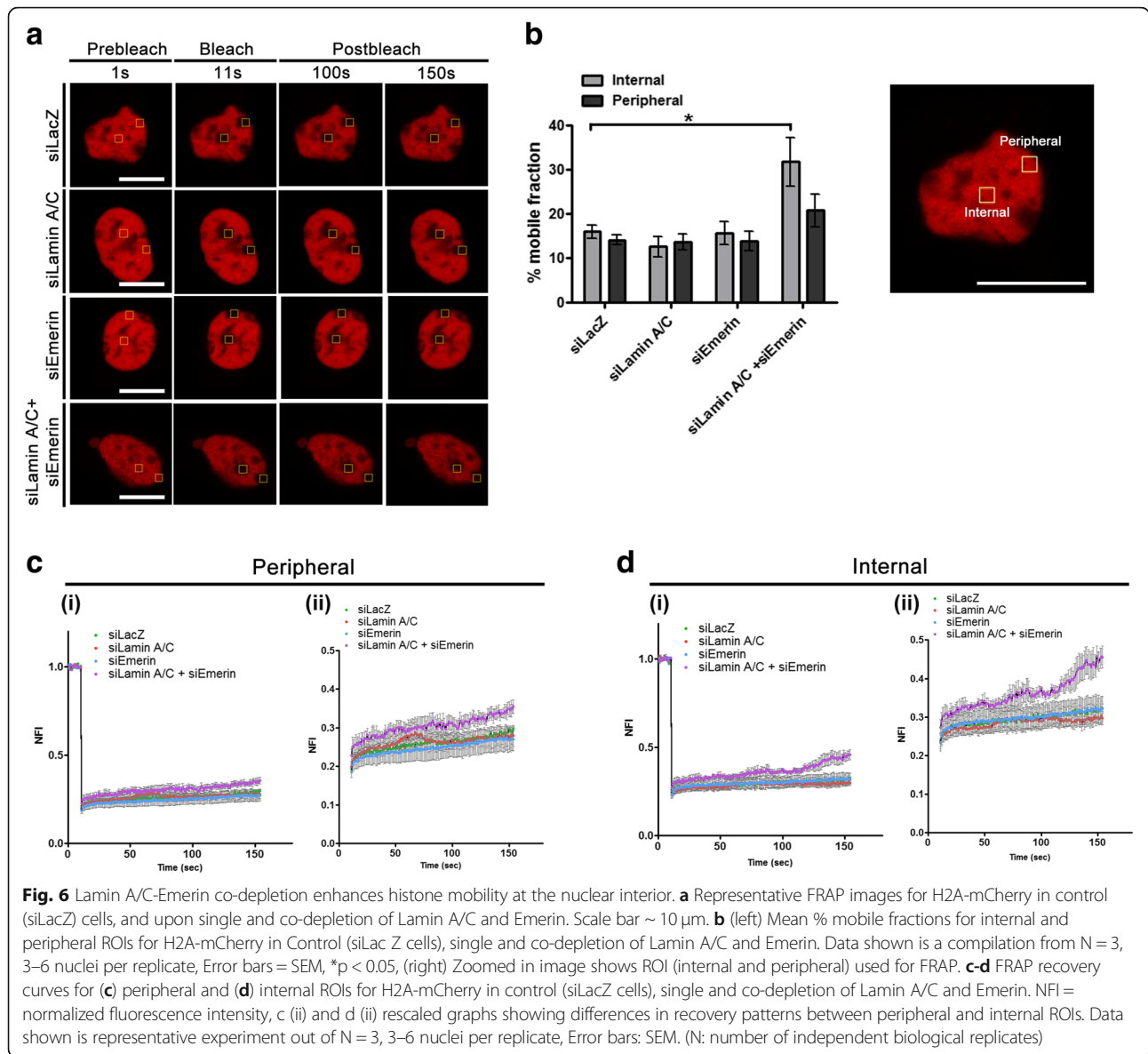
Fig. 6 Lamin A/C-Emerin co-depletion enhances histone mobility at the nuclear interior. **a** Representative FRAP images for H2A-mCherry in control (siLacZ) cells, and upon single and co-depletion of Lamin A/C and Emerin. Scale bar ~ 10 μm. **b** (left) Mean % mobile fractions for internal and peripheral ROIs for H2A-mCherry in Control (siLac Z cells), single and co-depletion of Lamin A/C and Emerin. Data shown is a compilation from N = 3, 3–6 nuclei per replicate, Error bars = SEM, *p < 0.05, (right) Zoomed in image shows ROI (internal and peripheral) used for FRAP. **c-d** FRAP recovery curves for (**c**) peripheral and (**d**) internal ROIs for H2A-mCherry in control (siLacZ cells), single and co-depletion of Lamin A/C and Emerin. NFI = normalized fluorescence intensity, c (ii) and d (ii) rescaled graphs showing differences in recovery patterns between peripheral and internal ROIs. Data shown is representative experiment out of N = 3, 3–6 nuclei per replicate, Error bars: SEM. (N: number of independent biological replicates)

Table 2 Median % Radial Distance of CT 7 and CT17 upon co-depletion of Lamin A/C and Emerin in DLD-1 cells

Chromosome/Gene Density	Experiment	%Radial Distance (R.D)
CT7 (17.45 genes/Mbp)	Untreated	71.69
	siLamin A/C	68.87
	siEmerin	73.35
	siLamin A/C + siEmerin	71.20
CT17 (29.30 genes/Mbp)	Untreated	61.43
	siLamin A/C	53.42[a] (*p* = 0.0202)
	siEmerin	62.00
	siLamin A/C + siEmerin	50.27[a] (*p* = 0.0137)

[a]: statistically significant

interior as compared to the nuclear periphery (Fig. 6). Furthermore, locations of chromosome territories proximal to the nuclear envelope were unaffected, owing to the presence of B type Lamins (Additional file 3b), despite the loss of Lamin A/C and Emerin proteins at the nuclear envelope.

Lamin A/C and Emerin modulate localization and activity of nuclear myosin 1

NM1 is dependent on Lamin A/C and Emerin for its nuclear localization (Fig. 2). Major chromatin remodeling events during transcription and independent short and long-range chromatin movements are modulated by NM1 [114]. Although the interaction between NM1 and Emerin is well established [62], the functional relevance of such an interaction and its impact on chromatin

Table 3 % Mobile fractions of H2A-mCherry upon co-depletion of Lamin A/C and Emerin

Experiment	Mean % Mobile Fraction (± SEM)	
	Internal	Peripheral
siLacZ	16.01 ± 1.48	14.12 ± 1.12
siLamin A/C	12.58 ± 2.32	13.58 ± 1.81
siEmerin	15.57 ± 2.61	13.80 ± 2.16
siLamin A/C + siEmerin	31.75 ± 5.46[a] ($p = 0.02381$)	20.82 ± 3.71

[a]: statistically significant

organization remains unclear. Lamin A/C modulates the localization of NM1 in an Emerin dependent manner in the nucleus (Fig. 2). Moreover, NM1 associates with gene rich chromosome territories to a greater extent than gene poor chromosome territories [68, 80] suggesting an enhanced requirement for binding and activity of NM1 with gene rich chromosome territories. It is likely that NM1 activity is altered upon the depletion of Lamin A/C and Emerin, as the inhibition of NM1 activity via drug treatment (BDM), rescues enhanced chromatin mobility in Lamin A/C-Emerin co-depleted cells to basal
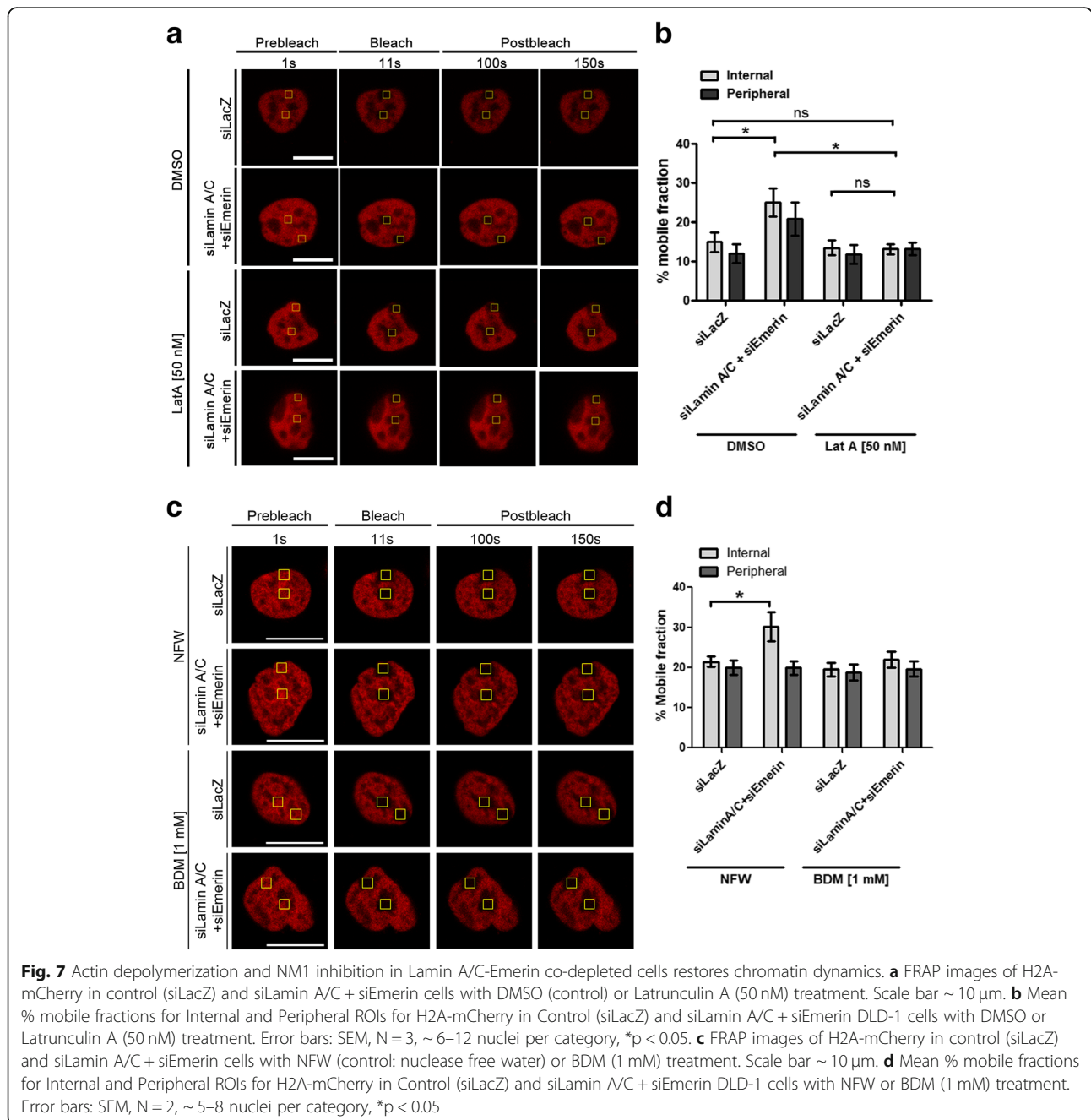

Fig. 7 Actin depolymerization and NM1 inhibition in Lamin A/C-Emerin co-depleted cells restores chromatin dynamics. **a** FRAP images of H2A-mCherry in control (siLacZ) and siLamin A/C + siEmerin cells with DMSO (control) or Latrunculin A (50 nM) treatment. Scale bar ~ 10 μm. **b** Mean % mobile fractions for Internal and Peripheral ROIs for H2A-mCherry in Control (siLacZ) and siLamin A/C + siEmerin DLD-1 cells with DMSO or Latrunculin A (50 nM) treatment. Error bars: SEM, N = 3, ~ 6–12 nuclei per category, *p < 0.05. **c** FRAP images of H2A-mCherry in control (siLacZ) and siLamin A/C + siEmerin cells with NFW (control: nuclease free water) or BDM (1 mM) treatment. Scale bar ~ 10 μm. **d** Mean % mobile fractions for Internal and Peripheral ROIs for H2A-mCherry in Control (siLacZ) and siLamin A/C + siEmerin DLD-1 cells with NFW or BDM (1 mM) treatment. Error bars: SEM, N = 2, ~ 5–8 nuclei per category, *p < 0.05

Table 4 % Mobile fractions of H2A-mCherry upon Latrunculin A treatment of Lamin A/C and Emerin co-depleted cells

Experiment	Mean % Mobile Fraction (± SEM)	
	Internal	Peripheral
siLacZ + DMSO	14.94 ± 2.41	11.97 ± 2.44
siLamin A/C + siEmerin + DMSO	25.12 ± 3.60[a] ($p = 0.03717$)	20.84 ± 4.12
siLacZ + Lat A [50 nM]	13.49 ± 1.85	11.81 ± 2.35
siLamin A/C + siEmerin + Lat A [50 nM]	13.14 ± 1.32	13.19 ± 1.60

[a]: statistically significant

levels (Fig. 7d). We speculate that Lamin A/C and Emerin co-regulate the sub-cellular organization and activity of NM1. Since NM1 is enriched on active chromatin, the loss of NM1 function is likely to impact chromatin preferentially near the nuclear interior than heterochromatin proximal to the nuclear envelope (Fig. 9).

Actin reorganization modulates chromatin dynamics

Lamin A/C-Emerin co-depletion perturbs cytoskeletal organization as revealed by enhanced actin bundling, while Lamin A/C and Emerin knockdowns, redistribute NM1 foci into the nucleus (Figs. 2 and 3). Actin and NM1 are independently involved in modulating chromatin dynamics, required for long range chromatin movements. Reorganization of perinuclear F-actin reduces intranuclear G-actin [60]. RNA Polymerase II utilizes G actin for transcription [79]. We speculate that the reorganization of perinuclear F-actin upon Lamin A/C-Emerin co-depletion affects the organization of G-actin in the nucleus. This is consistent with a reduction in the levels of nuclear actin in Lamin A/C-Emerin co-depleted cells (Fig. 3c-e). Such a disruption of the actin network may primarily impact the activity and organization of euchromatin, since G-actin is required for remodeling transcriptionally active chromatin. Of note, enhanced chromatin mobility in the nuclear interior upon Lamin A/C and Emerin co-depletion was rescued upon Latrunculin A treatment, further underscoring the role of actin in modulating chromatin organization (Fig. 7b). Interestingly, perturbing actin organization affects the topology of chromosome territories and reduces gene loci dynamics at the nuclear interior rather than the periphery [115, 116]. This suggests the involvement of actin

organization in maintaining chromatin organization and dynamics in the nucleus [116].

Taken together, we surmise that Lamin A/C and Emerin partner to modulate chromatin organization via actin and nuclear myosin 1. Surprisingly, the positions of gene poor chromosome territories proximal to the nuclear lamina were unaffected upon co-depletion of Lamin A/C and Emerin (Figs. 4 and 5). We speculate that while Lamin A/C-Emerin and their interactors distinctively regulate chromatin toward the nuclear interior, protein complexes associated with B type lamins such as LBR, HP1α among others, maintain chromatin organization closer to the nuclear periphery. Thus, Lamins and their sub-interactome maintain and fine-tune the spatial organization of chromosome territories in the interphase nucleus. Additionally, Lamin A/C and Emerin could also partner to maintain the organization and function of gene loci, since the loss of Lamin A/C or Emerin perturbs expression and localization of genes in the nucleus (Fig. 8). In summary, Emerin and Lamin A/C partner to maintain the spatio-functional organization of chromatin and its dynamics in the nucleus.

The functional significance of the mislocalization of gene rich chromosome territories upon Lamin A/C and Emerin depletion is unclear and remains to be investigated. Mislocalization of chromosome territories is likely to reorganize Topologically Associated Domains (TADs) and Lamina Associated Domains (LADs) [33, 117, 118]. Hi-C analyses might reveal the nature of chromatin contacts regulated by Lamin A/C-Emerin and the NM1-Actin sub-complex. An integrated study of chromatin conformation and its correlation with gene expression through single cell transcriptomics and high

Table 5 % Mobile fractions of H2A-mCherry upon BDM treatment of Lamin A/C and Emerin co-depleted cells

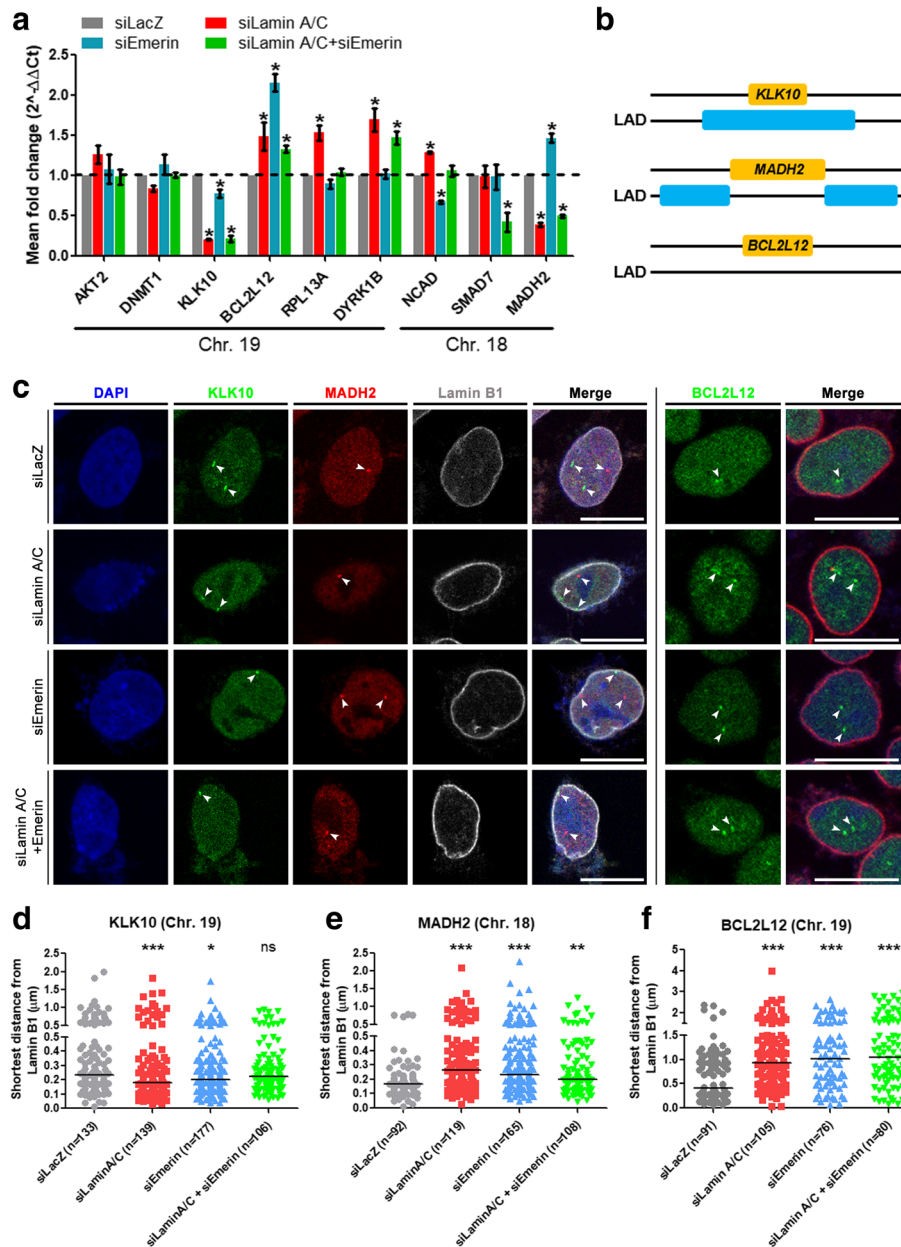| Experiment	Mean % Mobile Fraction (± SEM)	
	Internal	Peripheral
siLacZ + NFW	21.48 ± 1.36	20.05 ± 1.79
siLamin A/C + siEmerin + NFW	30.17 ± 3.60[a] ($p = 0.04218$)	19.92 ± 1.73
siLacZ + BDM [1 mM]	19.53 ± 1.73	18.78 ± 1.97
siLamin A/C + siEmerin + BDM [1 mM]	21.99 ± 1.99	19.64 ± 1.93

[a]: statistically significant

Fig. 8 Spatial positions of gene loci are altered upon Lamin A/C and Emerin depletion. **a** qRT-PCR showing expression changes in candidate genes from chromosome 18 and 19 upon treatment of DLD-1 cells with siLacZ (control), siLamin A/C, siEmerin and siLamin A/C + siEmerin. Expression levels were first normalized to internal control GAPDH and then to siLacZ. Pooled data from N = 3 independent biological replicates, *p < 0.05. **b** Schematic representation of the Lamina Associated Domain (LAD) status of KLK10, SMAD2/MADH2 and BCL2L12. Blue bars represent the Lamin B1 Dam-ID data from Netherlands Cancer Institute (NKI). Snapshots from the UCSC Genome Browser have been provided in Additional files 6 and 7. **c** Representative mid-optical sections from confocal z- stacks of Immuno-3D FISH for KLK10 (Chr. 19), MADH2 (Chr. 18) and BCL2L12 (Chr. 19) gene loci in DLD-1 cells treated with siLacZ (control), siLamin A/C, siEmerin and siLamin A/C+Emerin. Nuclear envelope was demarcated by immunostaining for Lamin B1. **d** Shortest distance of KLK10 (Chr. 19) gene loci from Lamin B1 immunostaining in DLD-1 cells treated with siLacZ (control, Median (M), M = 0.233 μm), siLamin A/C (M = 0.181 μm), siEmerin (M = 0.201 μm) and siLamin A/C + siEmerin (M = 0.223 μm). **e** Shortest distance of MADH2 (Chr. 18) gene loci from Lamin B1 immunostaining in DLD-1 cells treated with siLacZ (control, M = 0.169 μm), siLamin A/C (M = 0.266 μm), siEmerin (M = 0.235 μm) and siLamin A/C + siEmerin (M = 0.199 μm). **f** Shortest distance of BCL2L12 (Chr. 19) gene loci from Lamin B1 immunostaining in DLD-1 cells treated with siLacZ (control, M = 0.413 μm), siLamin A/C (M = 0.929 μm), siEmerin (M = 1.02 μm) and siLamin A/C + siEmerin (M = 1.05 μm). **d**-**f**, Horizontal bar - Median (M): Pooled data from N = 2 independent biological replicates, *** p < 0.001, ** p < 0.01, * p < 0.05. Scale bar ~ 10 μm
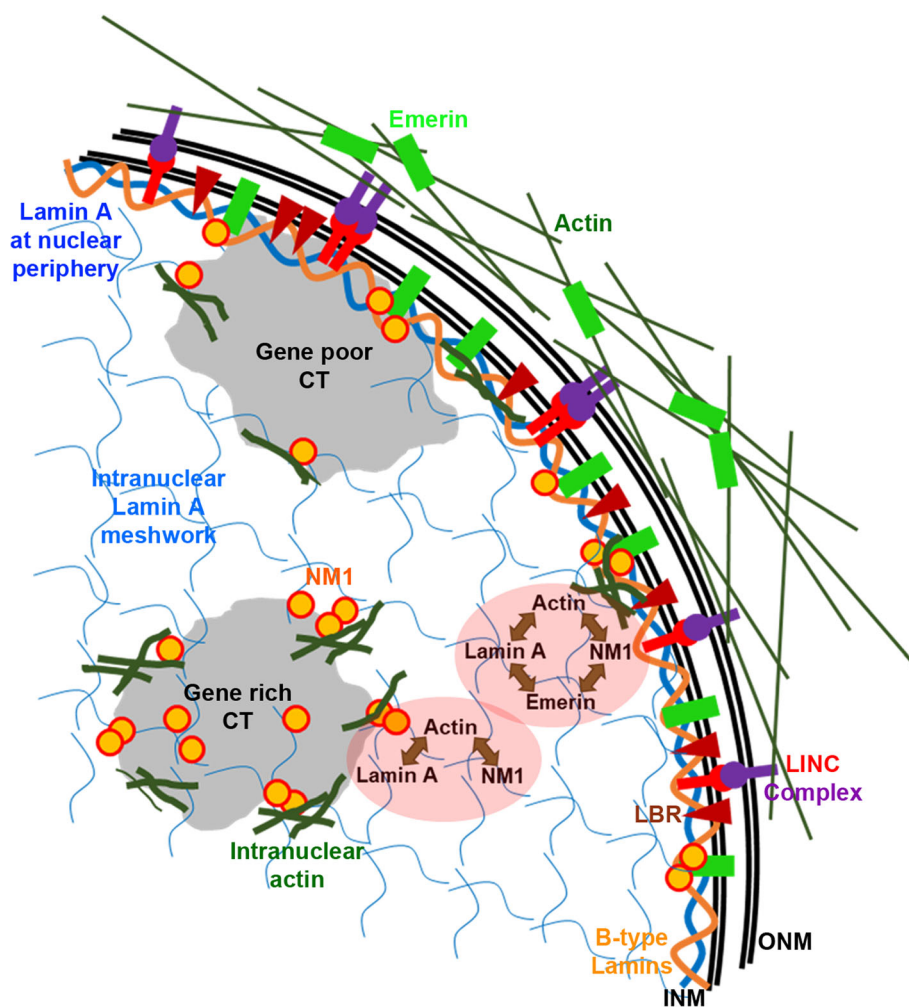
Fig. 9 Schematic model suggesting a role for Lamin A/C and Emerin in regulating cytoskeletal and chromatin dynamics in the interphase nucleus. Lamin A/C and Emerin in association with actin and nuclear myosin (NM1), maintains cytoskeletal organization, which when destabilized, perturbs genome organization

resolution imaging of single cells, may unravel the mechanistic underpinnings of how the cytoskeleton and the nucleus communicate with one another to enrich for specific and unique chromatin conformations, that in turn manifest into context specific transcriptional outputs, in a cell type and tissue specific manner.

Conclusions

In conclusion, these studies reveal that Lamin A/C and Emerin partner to modulate genome organization via their cytoskeletal interactors – actin and NM1. Co-depletion of Lamin A/C and Emerin increases cytoplasmic actin stress fibers, decreases nuclear actin levels and potentially alters NM1 activity in the nucleus. This impacts genome organization as Lamin A/C and Emerin co-depletion enhances chromatin mobility toward the nuclear interior which was restored to basal levels upon

NM1 inhibition or actin depolymerization. Impact on the genome was further reiterated by the mislocalization of chromosome territories upon Lamin A/C-Emerin co-depletion, and deregulation of gene expression levels of candidate genes - KLK10, BCL2L12 and MADH2, that differentially associate with the nuclear envelope, largely consistent with their Lamina Associated Domain (LAD) status. This study reinforces the intricate crosstalk between the cytoskeleton and the nucleus, orchestrated by Lamin A/C and Emerin that modulate cytoskeletal factors – actin and NM1.

Methods

Cell culture

DLD-1 colorectal adenocarcinoma cells were cultured in RPMI 1640 with 10% Fetal Bovine Serum, Penicillin (100 U/mL) and Streptomycin (100 μg/mL) (Invitrogen,

Thermo Fischer Scientific, MA, USA) and were a gift from Dr. Thomas Ried, NCI/NIH, Bethesda, USA. Cells were routinely karyotyped to ascertain chromosomal stability and modal number of 44–46 chromosomes across multiple independent passages (Additional file 3a). Experiments were typically confined to cells cultured within the first 8–15 passages.

siRNA transfection
siRNAs used for Lamin A/C and Emerin are siLMNA/C: 5′-CAGUCUGCUGAGAGGAACA-3′, siEMD1: 5′-UCU GACUUGAAUUCGACUA-3′ and siEMD2: 5′-UCCC AGAUGCUGACGCUUU-3′, non-targeting siRNA control siLACZ: 5′-CGUACGCGGAAUACUUCGA-3′. siRNA transfection mix was prepared using Lipofectamine RNAi-max in Opti-MEM (Invitrogen, 13,778,150 and 31,985–070 respectively), ~ 0.2 X 10^6 cells were plated with siRNA transfection mix for EMD (EMD1 and EMD2 siRNA oligos at 50 nM each) on day 1. Cells were pulsed with EMD1 and EMD2 oligos (50 nM each) for single EMD knockdown (Kd) and EMD1 + EMD2 (50 nM each) + LMNA/C (100 nM) for co-depletion (day 2). Single LMNA Kd was set up with LMNA/C siRNA (100 nM) (day 2). Knockdown continued for 48 h, followed by a change of media (day 4). Cells were harvested after 24 h (day 5).

Western blotting
DLD-1 cells were lysed with Radio Immuno Precipitation Assay (RIPA) Buffer. Heat denatured protein samples were resolved on 10% acrylamide-bisacrylamide gel, transferred to an activated PVDF membrane (90 V for 90 min), blocked in 5% non-fat dried milk - 1 h/RT and incubated in primary antibodies prepared in 0.5% milk in 1X TBST. Primary antibodies used are as follows - anti- Lamin A (ab26300, 1:1000), anti-Lamin A/C (Jol2 ab40567, 1:200), anti-Actin (ab3280, 1:400), anti-Emerin (06–1052, 1:3000), anti-Emerin (ab40688, 1:1500), anti-MYO1C (ab51261, 1:1000) and anti-GAPDH (G9545, 1:5000). Secondary antibodies - anti-mouse IgG-HRP (GE, IL, USA- NA9310V, 1:5000) and anti-rabbit IgG-HRP (GE, IL, USA- NA9340V, 1:10000). Blots were incubated in primary antibody overnight at 4 °C and secondary antibodies for 1 h at RT respectively. Chemiluminescent substrates were used to develop the blots (GE ECL Prime (89168–782)).

Immunofluorescence assay
DLD-1 cells were seeded on coverslips and siRNA or drug treatments were performed. Cells were washed with 1X Phosphate Buffered Saline (PBS) (2 X 5 min, RT) and fixed in 4% Paraformaldehyde (PFA) (in 1X PBS (pH 7.4)) for 10 min (RT), followed by two washes in 1X PBS washes. Cells were permeabilized in 0.5% Triton-X-100 (in 1X PBS) - 10 min, followed by 1X PBS washes (5 min, twice).

Immunostaining protocol was followed as per Ranade et al. [86]. Primary antibodies used are as follows - anti-Lamin A (ab26300, 1:750), anti-Lamin A/C (Jol2 ab40567, 1:50), anti-Emerin (ab14208, 1:250), anti-Emerin (sc-25284, 1:500), anti-MYO1C (ab51261, 1:75) and anti-Lamin B2 (ab8983, 1:400). Secondary antibodies used are as follows - anti-Rabbit Alexa 488 (A11034, 1:1000) and anti-Mouse Alexa 568 (A11004, 1:1000).

3-dimensional fluorescence in situ hybridization (3D-FISH)
Fixation 3D-FISH was performed as per standard protocols [86]. ***Hybridization*** Chromosome painting probes (Applied Spectral Imaging (ASI), Israel) were incubated at 37 °C for 5 min, denatured at 80 °C for 5 min, quick chilled on ice for 2 min and pre-annealed at 37 °C (~ 45 min). ~ 3–4 μl probe was applied to fixed cells on an 18 X 18 mm^2 coverslip, co-denatured at 80 °C for 5 min, and hybridized for 48 h at 37 °C. ***Detection*** Coverslips were washed in 50% FA/2X SSC (pH 7.4) - 3 X 5 min at 45 °C, 0.1X SSC - 3 X 5 min at 60 °C, rinsed in 0.1% Tween20/4X SSC, counterstained with DAPI (3 min at RT), gently washed in 2X SSC and mounted. ***Imaging*** Image acquisition was performed on a Zeiss LSM 710 confocal microscope (Carl Zeiss, Thornwood, NJ, USA) or Leica TCS SP8 confocal laser scanning microscope (Leica Microsystems, Wetzlar, Germany) with 63X Plan-Apochromat 1.4 NA oil immersion objective. Image acquisition: zoom factor 2.0, Z-stacked images of voxel size 0.132 μm X 0.132 μm X 0.34 μm, 512X512 pixels per frame using 8-bit pixel depth for each channel. Line averaging: 2.0 and images acquired sequentially in a three-channel mode.

Radial distance measurements of chromosome territories
3D radial distance measurements were performed using Image-Pro Plus (v 7.1). Single nuclei were cropped and subjected to 3D surface rendering followed by radial distance measurements of chromosome territories [86, 87].

Statistical analysis
Statistical analysis was performed using GraphPad Prism 5.0 and Microsoft Excel. Radial Distances (% R.D) of chromosome territories and distances of gene loci were compared using Mann Whitney sum-rank test. Comparisons between proportions of cells showing NM1 mislocalization and actin stress fiber aggregates were done using Fisher's exact test. Average mobile fractions were compared using unpaired Student's-t-test. The non-targeting control (siLacZ) served as a reference for analyses of each data set. A p-value < 0.05 was considered as statistically significant.

Fluorescence recovery after Photobleaching (FRAP) and analyses

Cells were grown on collagen (100 μg/ml) coated glass coverslips (22 X 22 mm²) placed on 35 mm petri dishes. Cells were transfected with H2A-mCherry construct (gift from Michael Davidson [Addgene plasmid # 55054]) for 24 h prior to photobleaching experiments. Cells were maintained in CO_2 independent Leibovitz L-15 medium (Gibco, 21083–027) during photobleaching. Images were acquired using a 63X oil immersion objective with NA 1.4, 3X digital zoom in a Zeiss LSM 710 confocal microscope. Two independent Regions of Interest (ROI) of 20px X 20px (1 pixel = 0.0879 μm) were used for bleaching - one ROI in the nuclear interior and other near the nuclear border. Photobleaching conditions - 561 nm laser line, 80% laser power for photobleaching (100 iterations), 10 scans of pre-bleach, image acquisition every 1 s. Post bleach acquisition was performed in the duration when the relative nuclear motion and displacement was minimum. Images were analyzed using Zen 2011 FRAP Analysis module and Normalized Fluorescence Intensity (NFI) was calculated as follows:

$$NFI = \frac{ROI1(t) - ROI3(t)}{ROI2(t) - ROI3(t)} \; X \; \frac{ROI2(t=0) - ROI3(t=0)}{ROI1(t=0) - ROI3(t=0)}$$

ROI1: fluorescence intensity - interior/peripheral ROI, ROI2: fluorescence intensity of a 20px X 20px region of the nucleus that was not subjected to photobleaching, and ROI3: fluorescence intensity of a 20px X 20px background region outside the nucleus. ROI1 (t) denotes the post-bleach fluorescence intensity at time t. ROI2 (t) and ROI3 (t) denote the same for unbleached ROI and background, respectively. ROI1 (t = 0) denotes the average pre-bleach fluorescence intensity. ROI2 (t = 0) and ROI3 (t = 0) denote the same for unbleached ROI and background, respectively. The NFI was plotted as a function of time to generate double normalized FRAP curves. Mobile fractions of H2A-mCherry were calculated as follows:

$$\%Mobile\ fraction = \frac{Ffinal - Fbleach}{Fprebleach - Fbleach} \times 100$$

Where, Ffinal is the NFI at maximum recovery (saturation), Fbleach is the NFI at the instant of bleaching and Fpre-bleach is the NFI before bleaching [119].

Actin depolymerization and NM1 inhibition for live imaging

siRNA mediated co-depletion of Lamin A/C and Emerin was performed as mentioned previously, and H2A-mCherry overexpression was carried out 24 h prior to photobleaching experiments. Leibovitz L-15 medium was added to the Lamin A/C-Emerin co-depleted cells

(and siLacZ control cells), followed by treatment with either 50 nM Latrunculin A or 1 mM BDM for 60 mins. FRAP and live imaging of cells was performed in the presence of the inhibitor for the next 45–60 min.

Co-immunoprecipitation

Co-immunoprecipitation was performed using Co-IP Lysis Buffer (50 mM Tris pH 8.0, 300 mM NaCl, 0.5% NP-40, 1X Protease Inhibitor Cocktail - Roche, Basel, Switzerland). Cells were lysed in Co-IP Lysis Buffer, incubated on ice (30 min) and centrifuged at 14000 rpm for 15 min at 4 °C. For Co-IP, 120 μg of lysate (each from Control and siLamin A/C cells) was pre-cleared using Protein G/A-Dynabeads (45 min at 4 °C). Primary antibody (anti-Emerin sc25284, anti-MYO1C ab51261) (1 μg) and normal mouse/rabbit IgG (1 μg) were added, followed by overnight incubation at 4 °C. Antigen-antibody complexes were captured (4 h at 4 °C) using 20 μl Protein G/A-Dynabeads (blocked previously with 0.5 mg/ml BSA in 1X PBS [30 min/4 °C]). Beads were washed six times with Co-IP Lysis buffer, boiled in 4X Laemmli, resolved on polyacrylamide gel and subjected to western blotting.

Preparation of nuclear and cytoplasmic extracts

REAP Protocol was followed [120].

Immuno-3D FISH

Fixation for 3-D ImmunoFISH DLD-1 cells growing on coverslips and subjected to Lamin A/C and Emerin knockdowns were treated with CSK buffer for 6.5 mins, followed by fixation using 4% PFA (pH = 7.2, PFA, Sigma, 158,127) for 12 mins at RT. After two washes in 1X PBS, cells were permeabilized in 0.5% Triton X-100 (in 1X PBS) for 15 mins, followed by incubation in 20% glycerol (in 1X PBS) for 45 mins. Cells were subjected to 5 freeze-thaw cycles in liquid nitrogen, followed by 3 washes in 1X PBS. Cells were denatured in 0.1 N HCl for 10 mins, followed by two washes in 50% FA-2X SSC (pH 7.4). Nuclei were stored in 50% FA-2X SSC (pH 7.4) at 4 °C overnight or until further use. ***Immunofluorescence Assay*** Cells fixed previously on coverslips were washed briefly using 1X PBS (5 min, once at RT). Blocking was performed in 1% BSA (Sigma, A2153) solution for 30 mins. The primary antibody Rabbit anti-Lamin B1 (ab16048, 1:1000) was diluted in 0.5% BSA and cells were incubated at RT for 90 min. Secondary antibody Goat anti-Rabbit Alexa-633 (A21070, 1:1000) diluted in 1X PBS-Triton X-100 (1X PBST) was applied to cells on coverslips at RT for 60 min. ***Hybridization and post-hybridization washes*** After the final 3 washes of 1X PBST, coverslips were stored in 1X PBST for 45 mins. Post-fixation was in 4% PFA for 7 mins and post-permeabilization in 0.5% Triton X-100 for 7 mins,

followed by 2 washes in 1X PBS and 2 washes in 50% FA-2X SSC. BAC clone RP11-380 M21 for MADH2, RP11-26P12 for KLK10 and RP11-264 M8 for BCL2L12 were purified using isolation protocol by Villalobos et al., optimized for 100 ml cultures [121]. Required amount of MADH2, KLK10 and BCL2L12 probe labelled with Texas Red and Rhodamine dUTPs respectively using Nick Translation Kit (Roche, following kit protocol) was incubated at 37 °C for 7 mins/750 rpm. Probe was denatured at 80 °C for 5 mins and quick chilled on ice for 2 mins. Pre-annealing was at 37 °C for 45 mins. Co-denaturation of MADH2, KLK10 and BCL2L12 probe and immunostained nuclei was at 80 °C for 7 mins, followed by hybridization in a moist sealed chamber at 37 °C for 48 h. Post hybridization washes were with 50% FA-2X SSC at 45 °C (3 washes/5 mins each) and 0.1X SSC at 60 °C (3 washes/5 mins each). Nuclei were counterstained with DAPI and mounted in Antifade. *Imaging* Image acquisition was performed on a Zeiss LSM 710 confocal microscope (Carl Zeiss, Thornwood, NJ, USA) with 63X Plan-Apochromat 1.4 NA oil immersion objective. Image acquisition: zoom factor 1.5, Z-stacked images of voxel size 0.18 μm X 0.18 μm X 0.34 μm, 512 X 512 pixels per frame using 8-bit pixel depth for each channel. Line averaging: 4.0 and images acquired sequentially in a three-channel mode.

Additional files

Additional file 1: (a) Immunostaining for Emerin (green), Lamin A/C (red) in untreated, siLamin A/C and siLamin A/C scrambled treated DLD-1 cells at the end of 48 h post Lamin A/C Kd. Scale bar ~ 10 μm. (b) Quantification of number of cells showing mislocalization of Emerin as an extranuclear aggregate in control and Lamin A/C kd cells, n = number of cells analysed, compiled data from N = 2 independent biological replicates. (c) Representative mid-optical section from confocal z-stacks of NM1 immunostaining in siLacZ, siLamin A/C, siEmerin and siLamin A/C + siEmerin treated DLD-1 cells, showing the localization of NM1 foci inside the nucleus. Scale bar ~ 10 μm. (TIF 3756 kb)

Additional file 2: (a) Representative western blot showing expression levels of NM1 in single and combined depletion of Lamin A/C and Emerin in DLD-1 cells. (b) Densitometric quantification of band intensities for NM1 in single and combined depletion of Lamin A/C and Emerin. Error bar: SEM, compiled data from N = 5 independent biological replicates. (c) Above: Co-IP using anti-Emerin antibody, probed for interaction with NM1 in control (siLacZ) and Lamin A/C depleted cells. Below: Western blot showing Lamin A/C depletion. Loading control: Actin (d) Densitometric quantification of band intensities for NM1 in Emerin pulldown upon Lamin A/C depletion. Both Emerin and NM1 levels were normalized to their respective inputs and the extent of NM1 pulled down with Emerin was further normalized to total Emerin pulldown. Error bar: SEM, compiled data from N = 3 independent biological replicates. (TIF 1956 kb)

Additional file 3: (a) Metaphase counts of DLD-1 cells consistently show pseudo-diploid chromosome numbers of 44–46. Scale bar ~ 10 μm. (b) Immunostaining for Lamin B2 (red) upon Lamin A/C and Emerin co-depletion in DLD-1 cells. Scale bar ~ 10 μm. (c) Representative western blot showing Actin levels in whole cell extract of DLD-1 cells with single and combined depletion of Lamin A/C-Emerin. (d) Densitometric

quantification of band intensities for Actin in whole cell extracts from cells with single and combined depletion of Lamin A/C-Emerin. Error bar: SEM, compiled data from N = 3 independent biological replicates, *p < 0.05. (TIF 3645 kb)

Additional file 4: (a-b) Dot scatter plots showing nuclear area (a) and volume (b) upon single and combined depletion of Lamin A/C and Emerin. Control - siLacZ treated cells, Horizontal bar: Median (M), n: number of nuclei, compiled data from N = 3 independent biological replicates. (c-d) Dot scatter plots showing CT18 area (c) and volume (d) upon single and combined depletion of Lamin A/C and Emerin. Control - siLacZ treated cells, Horizontal bar: Median (M), n: number of CTs, data compiled from N = 2 independent biological replicates. (e-f) Dot scatter plots showing CT19 area (e) and volume (f) upon single and combined depletion of Lamin A/C and Emerin. Control - siLacZ treated cells, Horizontal bar: Median (M), n: number of CTs, compiled data from N = 2 independent biological replicates. (g-h) Dot scatter plots showing CT7 area (g) and volume (h) upon single and combined depletion of Lamin A/C and Emerin. Control - Untreated cells (UT), Horizontal bar: Median (M), n: number of CTs, N = 1 (data from single experiment). (i-j) Dot scatter plots depicting CT17 area (i) and volume (j) upon single and combined depletion of Lamin A/C and Emerin. Control - Untreated cells (UT), Horizontal bar: Median (M), n: number of CTs, N = 1 (data from single experiment), *p < 0.05, **p < 0.01, ***p < 0.001. (TIF 3572 kb)

Additional file 5: (a) Phalloidin staining (green) performed on cells treated with 50 nM and 100 nM Latrunculin A for 90 min. DMSO treated and untreated cells were used as controls. Depolymerization of actin was ascertained using reduced phalloidin staining upon Lat A treatment. Scale bar ~ 10 μm. (b) FRAP performed on H2A-mCherry in control (DMSO) and Lat A (50 nM) treated DLD-1 cells. Two ROIs were used for the experiment – interior of the nucleus (Internal) and proximal to nuclear periphery (Peripheral), ~ 4–5 nuclei were assayed for recovery fractions in each condition per experiment. (c) Mean % mobile fraction for control (DMSO) and Lat A (50 nM) treated DLD-1 cells. No significant difference was detected for the mobile fractions of H2A-mCherry in either the intranuclear or peripheral pools upon Lat A treatment (50 nM, 90 min) (p > 0.05, Unpaired Student's t-test). Error bars: SEM, compiled data from N = 2 independent biological replicates. (TIF 2609 kb)

Additional file 6: (a-h) UCSC Genome Browser view for (a) KLK10, (b) MADH2/SMAD2, (c) AKT2, (d) DNMT1, (e) DYRK1B, (f) RPL13A, (g) NCAD/CDH2 and (h) SMAD7, also depicting the Lamina Associated Domains (NKI LAD track). (TIFF 2608 kb)

Additional file 7: (a) UCSC Genome Browser view for BCL2L12, depicting the Lamina Associated Domains (NKI LAD track). (b) Representative mid-optical sections from confocal z-stacks of Immuno-3D FISH for BCL2L12 (Chr. 19) gene loci in DLD-1 cells treated with siLacZ (control), siLamin A/C, siEmerin and siLamin A/C + siEmerin. Nuclear envelope was demarcated using immunostaining of Lamin B1. Scale bar ~ 10 μm. (TIFF 2263 kb)

Abbreviations
CT: Chromosome territory; LAD: Lamina Associated Domain; LEM-D: LEM(LAP2-Emerin-MAN1)-domain; RD: Radial distance

Availability of data and materials
All data generated or analysed during this study are included in this published article and its supplementary information files.

Authors' contributions
KS, DR, RP designed the experiments. DR, RP, MJ and SH performed the experiments. DR, RP and MJ analyzed the data. KS, DR and RP wrote the manuscript. All authors read and approved the final manuscript.

Ethics approval and consent to participate
Not applicable.

Consent for publication
Not applicable.

Competing interests
The authors declare that they have no competing interests.

Publisher's Note
Springer Nature remains neutral with regard to jurisdictional claims in published maps and institutional affiliations.

References
1. Cremer M, von Hase J, Volm T, Brero A, Kreth G, Walter J, et al. Non-random radial higher-order chromatin arrangements in nuclei of diploid human cells. Chromosom Res. 2001;9:541–67.
2. Croft JA, Bridger JM, Boyle S, Perry P, Teague P, Bickmore WA. Differences in the localization and morphology of chromosomes in the human nucleus. J Cell Biol. 1999;145:1119–31.
3. Kalhor R, Tjong H, Jayathilaka N, Alber F, Chen L. Genome architectures revealed by tethered chromosome conformation capture and population-based modeling. Nat Biotechnol. 2011;30:90–8. https://doi.org/10.1038/nbt.2057.
4. Lieberman-Aiden E, van Berkum NL, Williams L, Imakaev M, Ragoczy T, Telling A, et al. Comprehensive mapping of long-range interactions reveals folding principles of the human genome. Science. 2009;326:289–93. https://doi.org/10.1126/science.1181369.
5. Shimi T, Pfleghaar K, Kojima S, Pack C-G, Solovei I, Goldman AE, et al. The A- and B-type nuclear Lamin networks: microdomains involved in chromatin organization and transcription. Genes Dev. 2008;22:3409–21. https://doi.org/10.1101/gad.1735208.
6. Fisher DZ, Chaudhary N, Blobel G. cDNA sequencing of nuclear lamins a and C reveals primary and secondary structural homology to intermediate filament proteins. Proc Natl Acad Sci U S A. 1986;83:6450–4.
7. Zewe M, Höger TH, Fink T, Lichter P, Krohne G, Franke WW. Gene structure and chromosomal localization of the murine Lamin B2 gene. Eur J Cell Biol. 1991;56:342–50.
8. Shimi T, Kittisopikul M, Tran J, Goldman AE, Adam SA, Zheng Y, et al. Structural organization of nuclear lamins a, C, B1, and B2 revealed by superresolution microscopy. Mol Biol Cell. 2015;26:4075–86. https://doi.org/10.1091/mbc.E15-07-0461.
9. Constantinescu D, Gray HL, Sammak PJ, Schatten GP, Csoka AB. Lamin a/C expression is a marker of mouse and human embryonic stem cell differentiation. Stem Cells. 2006;24:177–85. https://doi.org/10.1634/stemcells.2004-0159.
10. Eckersley-Maslin MA, Bergmann JH, Lazar Z, Spector DL. Lamin a/C is expressed in pluripotent mouse embryonic stem cells. Nucleus. 2013;4:53–60. https://doi.org/10.4161/nucl.23384.
11. Melcer S, Hezroni H, Rand E, Nissim-Rafinia M, Skoultchi A, Stewart CL, et al. Histone modifications and Lamin a regulate chromatin protein dynamics in early embryonic stem cell differentiation. Nat Commun. 2012;3:910. https://doi.org/10.1038/ncomms1915.
12. Kim Y, Sharov AA, McDole K, Cheng M, Hao H, Fan C-M, et al. Mouse B-type lamins are required for proper organogenesis but not by embryonic stem cells. Science. 2011;334:1706–10. https://doi.org/10.1126/science.1211222.
13. Hozák P, Sasseville AM, Raymond Y, Cook PR. Lamin proteins form an internal nucleoskeleton as well as a peripheral lamina in human cells. J Cell Sci. 1995;108(Pt 2):635–44.
14. Moir RD, Yoon M, Khuon S, Goldman RD. Nuclear lamins a and B1: different pathways of assembly during nuclear envelope formation in living cells. J Cell Biol. 2000;151:1155–68.
15. Broers JL, Machiels BM, van Eys GJ, Kuijpers HJ, Manders EM, van Driel R, et al. Dynamics of the nuclear lamina as monitored by GFP-tagged A-type lamins. J Cell Sci. 1999;112(Pt 20):3463–75.
16. Bridger JM, Kill IR, O'Farrell M, Hutchison CJ. Internal Lamin structures within G1 nuclei of human dermal fibroblasts. J Cell Sci. 1993;104(Pt 2):297–306.
17. Sen Gupta A, Sengupta K. Lamin B2 modulates nucleolar morphology, dynamics, and function. Mol Cell Biol. 2017;37. https://doi.org/10.1128/MCB.00274-17.
18. Pochukalina GN, Ilicheva NV, Podgornaya OI, Voronin AP. Nucleolus-like body of mouse oocytes contains Lamin a and B and TRF2 but not actin and topo II. Mol Cytogenet. 2016;9:50. https://doi.org/10.1186/s13039-016-0259-3.
19. Fricker M, Hollinshead M, White N, Vaux D. Interphase nuclei of many mammalian cell types contain deep, dynamic, tubular membrane-bound invaginations of the nuclear envelope. J Cell Biol. 1997;136:531–44.
20. Kennedy BK, Barbie DA, Classon M, Dyson N, Harlow E. Nuclear organization of DNA replication in primary mammalian cells. Genes Dev. 2000;14:2855–68. https://doi.org/10.1101/gad.842600.
21. Butin-Israeli V, Adam SA, Jain N, Otte GL, Neems D, Wiesmüller L, et al. Role of Lamin b1 in chromatin instability. Mol Cell Biol. 2015;35:884–98. https://doi.org/10.1128/MCB.01145-14.
22. Spann TP, Goldman AE, Wang C, Huang S, Goldman RD. Alteration of nuclear Lamin organization inhibits RNA polymerase II-dependent transcription. J Cell Biol. 2002;156:603–8. https://doi.org/10.1083/jcb.200112047.
23. Shumaker DK, Solimando L, Sengupta K, Shimi T, Adam SA, Grunwald A, et al. The highly conserved nuclear Lamin Ig-fold binds to PCNA: its role in DNA replication. J Cell Biol. 2008;181:269–80. https://doi.org/10.1083/jcb.200708155.
24. Shimi T, Butin-Israeli V, Adam SA, Hamanaka RB, Goldman AE, Lucas CA, et al. The role of nuclear Lamin B1 in cell proliferation and senescence. Genes Dev. 2011;25:2579–93. https://doi.org/10.1101/gad.179515.111.
25. Glass CA, Glass JR, Taniura H, Hasel KW, Blevitt JM, Gerace L. The alpha-helical rod domain of human lamins a and C contains a chromatin binding site. EMBO J. 1993;12:4413–24.
26. Taniura H, Glass C, Gerace L. A chromatin binding site in the tail domain of nuclear lamins that interacts with core histones. J Cell Biol. 1995;131:33–44.
27. Glass JR, Gerace L. Lamins a and C bind and assemble at the surface of mitotic chromosomes. J Cell Biol. 1990;111:1047–57.
28. Lourim D, Krohne G. Chromatin binding and polymerization of the endogenous Xenopus egg lamins: the opposing effects of glycogen and ATP. J Cell Sci. 1998;111(Pt 24):3675–86.
29. Ye Q, Worman HJ. Interaction between an integral protein of the nuclear envelope inner membrane and human chromodomain proteins homologous to Drosophila HP1. J Biol Chem. 1996;271:14653–6.
30. Lee KK, Haraguchi T, Lee RS, Koujin T, Hiraoka Y, Wilson KL. Distinct functional domains in emerin bind Lamin a and DNA-bridging protein BAF. J Cell Sci. 2001;114(Pt 24):4567–73.
31. Dechat T, Korbei B, Vaughan OA, Vlcek S, Hutchison CJ, Foisner R. Lamina-associated polypeptide 2alpha binds intranuclear A-type lamins. J Cell Sci. 2000;113(Pt 19):3473–84.
32. Montes de Oca R, Shoemaker CJ, Gucek M, Cole RN, Wilson KL. Barrier-to-autointegration factor proteome reveals chromatin-regulatory partners. PLoS One. 2009;4:e7050. https://doi.org/10.1371/journal.pone.0007050.
33. Guelen L, Pagie L, Brasset E, Meuleman W, Faza MB, Talhout W, et al. Domain organization of human chromosomes revealed by mapping of nuclear lamina interactions. Nature. 2008;453:948–51. https://doi.org/10.1038/nature06947.
34. Pickersgill H, Kalverda B, de Wit E, Talhout W, Fornerod M, van Steensel B. Characterization of the Drosophila melanogaster genome at the nuclear lamina. Nat Genet. 2006;38:1005–14. https://doi.org/10.1038/ng1852.
35. Kind J, van Steensel B. Stochastic genome-nuclear lamina interactions: modulating roles of Lamin a and BAF. Nucleus. 2014;5:124–30. https://doi.org/10.4161/nucl.28825.
36. Zullo JM, Demarco IA, Piqué-Regi R, Gaffney DJ, Epstein CB, Spooner CJ, et al. DNA sequence-dependent compartmentalization and silencing of chromatin at the nuclear lamina. Cell. 2012;149:1474–87. https://doi.org/10.1016/j.cell.2012.04.035.

37. Towbin BD, González-Aguilera C, Sack R, Gaidatzis D, Kalck V, Meister P, et al. Step-wise methylation of histone H3K9 positions heterochromatin at the nuclear periphery. Cell. 2012;150:934–47. https://doi.org/10.1016/j.cell.2012.06.051.

38. Lund E, Oldenburg AR, Delbarre E, Freberg CT, Duband-Goulet I, Eskeland R, et al. Lamin a/C-promoter interactions specify chromatin state-dependent transcription outcomes. Genome Res. 2013;23:1580–9. https://doi.org/10.1101/gr.159400.113.

39. Meuleman W, Peric-Hupkes D, Kind J, Beaudry J-B, Pagie L, Kellis M, et al. Constitutive nuclear lamina-genome interactions are highly conserved and associated with a/T-rich sequence. Genome Res. 2013;23:270–80. https://doi.org/10.1101/gr.141028.112.

40. Mislow JMK, Holaska JM, Kim MS, Lee KK, Segura-Totten M, Wilson KL, et al. Nesprin-1alpha self-associates and binds directly to emerin and Lamin a in vitro. FEBS Lett. 2002;525:135–40.

41. Lombardi ML, Jaalouk DE, Shanahan CM, Burke B, Roux KJ, Lammerding J. The interaction between nesprins and sun proteins at the nuclear envelope is critical for force transmission between the nucleus and cytoskeleton. J Biol Chem. 2011;286:26743–53. https://doi.org/10.1074/jbc.M111.233700.

42. Yang L, Munck M, Swaminathan K, Kapinos LE, Noegel AA, Neumann S. Mutations in LMNA modulate the Lamin A--Nesprin-2 interaction and cause LINC complex alterations. PLoS One. 2013;8:e71850. https://doi.org/10.1371/journal.pone.0071850.

43. Libotte T, Zaim H, Abraham S, Padmakumar VC, Schneider M, Lu W, et al. Lamin a/C-dependent localization of Nesprin-2, a giant scaffolder at the nuclear envelope. Mol Biol Cell. 2005;16:3411–24. https://doi.org/10.1091/mbc.E04-11-1009.

44. Liang Y, Chiu PH, Yip KY, Chan SY. Subcellular localization of SUN2 is regulated by Lamin a and Rab5. PLoS One. 2011;6:e20507. https://doi.org/10.1371/journal.pone.0020507.

45. Ye Q, Callebaut I, Pezhman A, Courvalin JC, Worman HJ. Domain-specific interactions of human HP1-type chromodomain proteins and inner nuclear membrane protein LBR. J Biol Chem. 1997;272:14983–9.

46. Kubben N, Voncken JW, Demmers J, Calis C, van Almen G, Pinto Y, et al. Identification of differential protein interactors of Lamin a and progerin. Nucleus. 2010;1:513–25. https://doi.org/10.4161/nucl.1.6.13512.

47. Goldberg MW, Huttenlauch I, Hutchison CJ, Stick R. Filaments made from A- and B-type lamins differ in structure and organization. J Cell Sci. 2008;121(Pt 2):215–25. https://doi.org/10.1242/jcs.022020.

48. Turgay Y, Eibauer M, Goldman AE, Shimi T, Khayat M, Ben-Harush K, et al. The molecular architecture of lamins in somatic cells. Nature. 2017;543:261–4. https://doi.org/10.1038/nature21382.

49. Xie W, Chojnowski A, Boudier T, Lim JSY, Ahmed S, Ser Z, et al. A-type Lamins form distinct filamentous networks with differential nuclear pore complex associations. Curr Biol. 2016;26:2651–8. https://doi.org/10.1016/j.cub.2016.07.049.

50. Dechat T, Gesson K, Foisner R. Lamina-independent lamins in the nuclear interior serve important functions. Cold Spring Harb Symp Quant Biol. 2010;75:533–43. https://doi.org/10.1101/sqb.2010.75.018.

51. Naetar N, Ferraioli S, Foisner R. Lamins in the nuclear interior - life outside the lamina. J Cell Sci. 2017;130:2087–96. https://doi.org/10.1242/jcs.203430.

52. Amendola M, van Steensel B. Nuclear lamins are not required for lamina-associated domain organization in mouse embryonic stem cells. EMBO Rep. 2015;16:610–7. https://doi.org/10.15252/embr.201439789.

53. Wheeler MA, Ellis JA. Molecular signatures of Emery-Dreifuss muscular dystrophy. Biochem Soc Trans. 2008;36(Pt 6):1354–8. https://doi.org/10.1042/BST0361354.

54. McCord RP, Nazario-Toole A, Zhang H, Chines PS, Zhan Y, Erdos MR, et al. Correlated alterations in genome organization, histone methylation, and DNA-Lamin a/C interactions in Hutchinson-Gilford progeria syndrome. Genome Res. 2013;23:260–9. https://doi.org/10.1101/gr.138032.112.

55. Taimen P, Pfleghaar K, Shimi T, Möller D, Ben-Harush K, Erdos MR, et al. A progeria mutation reveals functions for Lamin a in nuclear assembly, architecture, and chromosome organization. Proc Natl Acad Sci U S A. 2009;106:20788–93. https://doi.org/10.1073/pnas.0911895106.

56. Mewborn SK, Puckelwartz MJ, Abuisneineh F, Fahrenbach JP, Zhang Y, MacLeod H, et al. Altered chromosomal positioning, compaction, and gene expression with a Lamin a/C gene mutation. PLoS One. 2010;5:e14342. https://doi.org/10.1371/journal.pone.0014342.

57. Meaburn KJ, Levy N, Toniolo D, Bridger JM. Chromosome positioning is largely unaffected in lymphoblastoid cell lines containing emerin or A-type Lamin mutations. Biochem Soc Trans. 2005;33(Pt 6):1438–40. https://doi.org/10.1042/BST20051438.

58. Meaburn KJ, Cabuy E, Bonne G, Levy N, Morris GE, Novelli G, et al. Primary laminopathy fibroblasts display altered genome organization and apoptosis. Aging Cell. 2007;6:139–53. https://doi.org/10.1111/j.1474-9726.2007.00270.x.

59. Guilluy C, Osborne LD, Van Landeghem L, Sharek L, Superfine R, Garcia-Mata R, et al. Isolated nuclei adapt to force and reveal a mechanotransduction pathway in the nucleus. Nat Cell Biol. 2014;16:376–81. https://doi.org/10.1038/ncb2927.

60. Le HQ, Ghatak S, Yeung C-YC, Tellkamp F, Günschmann C, Dieterich C, et al. Mechanical regulation of transcription controls Polycomb-mediated gene silencing during lineage commitment. Nat Cell Biol. 2016;18:864–75. https://doi.org/10.1038/ncb3387.

61. Pradhan R, Ranade D, Sengupta K. Emerin modulates spatial organization of chromosome territories in cells on softer matrices. Nucleic Acids Res. 2018;46:5561–86. https://doi.org/10.1093/nar/gky288.

62. Holaska JM, Wilson KL. An emerin "proteome": purification of distinct emerin-containing complexes from HeLa cells suggests molecular basis for diverse roles including gene regulation, mRNA splicing, signaling, mechanosensing, and nuclear architecture. Biochemistry. 2007;46:8897–908. https://doi.org/10.1021/bi602636m.

63. Simon DN, Zastrow MS, Wilson KL. Direct actin binding to A- and B-type Lamin tails and actin filament bundling by the Lamin a tail. Nucleus. 2010;1:264–72. https://doi.org/10.4161/nucl.1.3.11799.

64. Pestic-Dragovich L, Stojiljkovic L, Philimonenko AA, Nowak G, Ke Y, Settlage RE, et al. A myosin I isoform in the nucleus. Science. 2000;290:337–41. https://doi.org/10.1126/science.290.5490.337.

65. Fomproix N, Percipalle P. An actin-myosin complex on actively transcribing genes. Exp Cell Res. 2004;294:140–8. https://doi.org/10.1016/j.yexcr.2003.10.028.

66. Chuang C-H, Carpenter AE, Fuchsova B, Johnson T, de Lanerolle P, Belmont AS. Long-range directional movement of an interphase chromosome site. Curr Biol. 2006;16:825–31. https://doi.org/10.1016/j.cub.2006.03.059.

67. Percipalle P, Fomproix N, Cavellán E, Voit R, Reimer G, Krüger T, et al. The chromatin remodelling complex WSTF-SNF2h interacts with nuclear myosin 1 and has a role in RNA polymerase I transcription. EMBO Rep. 2006;7:525–30. https://doi.org/10.1038/sj.embor.7400657.

68. Kulashreshtha M, Mehta IS, Kumar P, Rao BJ. Chromosome territory relocation during DNA repair requires nuclear myosin 1 recruitment to chromatin mediated by Υ-H2AX signaling. Nucleic Acids Res. 2016;44:8272–91. https://doi.org/10.1093/nar/gkw573.

69. Toh KC, Ramdas NM, Shivashankar GV. Actin cytoskeleton differentially alters the dynamics of Lamin a, HP1α and H2B core histone proteins to remodel chromatin condensation state in living cells. Integr Biol (Camb). 2015;7:1309–17. https://doi.org/10.1039/c5ib00027k.

70. Ramdas NM, Shivashankar GV. Cytoskeletal control of nuclear morphology and chromatin organization. J Mol Biol. 2015;427:695–706. https://doi.org/10.1016/j.jmb.2014.09.008.

71. Mehta IS, Amira M, Harvey AJ, Bridger JM. Rapid chromosome territory relocation by nuclear motor activity in response to serum removal in primary human fibroblasts. Genome Biol. 2010;11:R5. https://doi.org/10.1186/gb-2010-11-1-r5.

72. Mehta IS, Elcock LS, Amira M, Kill IR, Bridger JM. Nuclear motors and nuclear structures containing A-type lamins and emerin: is there a functional link? Biochem Soc Trans. 2008;36(Pt 6):1384–8. https://doi.org/10.1042/BST0361384.

73. Holaska JM, Kowalski AK, Wilson KL. Emerin caps the pointed end of actin filaments: evidence for an actin cortical network at the nuclear inner membrane. PLoS Biol. 2004;2:E231. https://doi.org/10.1371/journal.pbio.0020231.

74. Vartiainen MK, Guettler S, Larijani B, Treisman R. Nuclear actin regulates dynamic subcellular localization and activity of the SRF cofactor MAL. Science. 2007;316:1749–52. https://doi.org/10.1126/science.1141084.

75. Ho CY, Jaalouk DE, Vartiainen MK, Lammerding J. Lamin a/C and emerin regulate MKL1-SRF activity by modulating actin dynamics. Nature. 2013;497:507–11. https://doi.org/10.1038/nature12105.

76. Manilal S, Nguyen TM, Sewry CA, Morris GE. The Emery-Dreifuss muscular dystrophy protein, emerin, is a nuclear membrane protein. Hum Mol Genet. 1996;5:801–8.

77. Ostlund C, Ellenberg J, Hallberg E, Lippincott-Schwartz J, Worman HJ. Intracellular trafficking of emerin, the Emery-Dreifuss muscular dystrophy protein. J Cell Sci. 1999;112(Pt 11):1709–19.

78. Khanna N, Hu Y, Belmont AS. HSP70 transgene directed motion to nuclear speckles facilitates heat shock activation. Curr Biol. 2014;24:1138–44. https://doi.org/10.1016/j.cub.2014.03.053.

Ranade *et al. BMC Molecular and Cell Biology*   (2019) 20:11

Page 20 of 20

79. Qi T, Tang W, Wang L, Zhai L, Guo L, Zeng X. G-actin participates in RNA polymerase II-dependent transcription elongation by recruiting positive transcription elongation factor b (P-TEFb). J Biol Chem. 2011;286:15171–81. https://doi.org/10.1074/jbc.M110.184374.

80. Almuzzaini B, Sarshad AA, Farrants A-KÖ, Percipalle P. Nuclear myosin 1 contributes to a chromatin landscape compatible with RNA polymerase II transcription activation. BMC Biol. 2015;13:35. https://doi.org/10.1186/s12915-015-0147-z.

81. Venit T, Kalendová A, Petr M, Dzijak R, Pastorek L, Rohožková J, et al. Nuclear myosin I regulates cell membrane tension. Sci Rep. 2016;6:30864. https://doi.org/10.1038/srep30864.

82. Vaughan A, Alvarez-Reyes M, Bridger JM, Broers JL, Ramaekers FC, Wehnert M, et al. Both emerin and Lamin C depend on Lamin a for localization at the nuclear envelope. J Cell Sci. 2001;114(Pt 14):2577–90.

83. Ye J, Zhao J, Hoffmann-Rohrer U, Grummt I. Nuclear myosin I acts in concert with polymeric actin to drive RNA polymerase I transcription. Genes Dev. 2008;22:322–30. https://doi.org/10.1101/gad.455908.

84. Tojkander S, Gateva G, Lappalainen P. Actin stress fibers--assembly, dynamics and biological roles. J Cell Sci. 2012;125(Pt 8):1855–64. https://doi.org/10.1242/jcs.098087.

85. Lammerding J, Hsiao J, Schulze PC, Kozlov S, Stewart CL, Lee RT. Abnormal nuclear shape and impaired mechanotransduction in emerin-deficient cells. J Cell Biol. 2005;170:781–91. https://doi.org/10.1083/jcb.200502148.

86. Ranade D, Koul S, Thompson J, Prasad KB, Sengupta K. Chromosomal aneuploidies induced upon Lamin B2 depletion are mislocalized in the interphase nucleus. Chromosoma. 2017;126:223–44. https://doi.org/10.1007/s00412-016-0580-y.

87. Tanabe H, Müller S, Neusser M, von Hase J, Calcagno E, Cremer M, et al. Evolutionary conservation of chromosome territory arrangements in cell nuclei from higher primates. Proc Natl Acad Sci U S A. 2002;99:4424–9. https://doi.org/10.1073/pnas.072618599.

88. Cremer M, Küpper K, Wagler B, Wizelman L, von Hase J, Weiland Y, et al. Inheritance of gene density-related higher order chromatin arrangements in normal and tumor cell nuclei. J Cell Biol. 2003;162:809–20. https://doi.org/10.1083/jcb.200304096.

89. Bošković A, Eid A, Pontabry J, Ishiuchi T, Spiegelhalter C, Raghu Ram EVS, et al. Higher chromatin mobility supports totipotency and precedes pluripotency in vivo. Genes Dev. 2014;28:1042–7. https://doi.org/10.1101/gad.238881.114.

90. Dahl KN, Ribeiro AJS, Lammerding J. Nuclear shape, mechanics, and mechanotransduction. Circ Res. 2008;102:1307–18. https://doi.org/10.1161/CIRCRESAHA.108.173989.

91. Swift J, Discher DE. The nuclear lamina is mechano-responsive to ECM elasticity in mature tissue. J Cell Sci. 2014;127 Pt 14:3005–15. https://doi.org/10.1242/jcs.149203.

92. Swift J, Ivanovska IL, Buxboim A, Harada T, Dingal PCDP, Pinter J, et al. Nuclear Lamin-a scales with tissue stiffness and enhances matrix-directed differentiation. Science. 2013;341:1240104. https://doi.org/10.1126/science.1240104.

93. Heessen S, Fornerod M. The inner nuclear envelope as a transcription factor resting place. EMBO Rep. 2007;8:914–9. https://doi.org/10.1038/sj.embor.7401075.

94. Markiewicz E, Tilgner K, Barker N, van de Wetering M, Clevers H, Dorobek M, et al. The inner nuclear membrane protein emerin regulates beta-catenin activity by restricting its accumulation in the nucleus. EMBO J. 2006;25:3275–85. https://doi.org/10.1038/sj.emboj.7601230.

95. Capanni C, Mattioli E, Columbaro M, Lucarelli E, Parnaik VK, Novelli G, et al. Altered pre-Lamin a processing is a common mechanism leading to lipodystrophy. Hum Mol Genet. 2005;14:1489–502. https://doi.org/10.1093/hmg/ddi158.

96. Ivorra C, Kubicek M, González JM, Sanz-González SM, Alvarez-Barrientos A, O'Connor J-E, et al. A mechanism of AP-1 suppression through interaction of c-Fos with Lamin a/C. Genes Dev. 2006;20:307–20. https://doi.org/10.1101/gad.349506.

97. Johnson BR, Nitta RT, Frock RL, Mounkes L, Barbie DA, Stewart CL, et al. A-type lamins regulate retinoblastoma protein function by promoting subnuclear localization and preventing proteasomal degradation. Proc Natl Acad Sci U S A. 2004;101:9677–82. https://doi.org/10.1073/pnas.0403250101.

98. Imai S, Nishibayashi S, Takao K, Tomifuji M, Fujino T, Hasegawa M, et al. Dissociation of Oct-1 from the nuclear peripheral structure induces the cellular aging-associated collagenase gene expression. Mol Biol Cell. 1997;8:2407–19.

99. Dreuillet C, Tillit J, Kress M, Ernoult-Lange M. In vivo and in vitro interaction between human transcription factor MOK2 and nuclear Lamin a/C. Nucleic Acids Res. 2002;30:4634–42.

100. Haraguchi T, Holaska JM, Yamane M, Koujin T, Hashiguchi N, Mori C, et al. Emerin binding to Btf, a death-promoting transcriptional repressor, is disrupted by a missense mutation that causes Emery-Dreifuss muscular dystrophy. Eur J Biochem. 2004;271:1035–45.

101. Holaska JM, Rais-Bahrami S, Wilson KL. Lmo7 is an emerin-binding protein that regulates the transcription of emerin and many other muscle-relevant genes. Hum Mol Genet. 2006;15:3459–72. https://doi.org/10.1093/hmg/ddl423.

102. Holaska JM, Lee KK, Kowalski AK, Wilson KL. Transcriptional repressor germ cell-less (GCL) and barrier to autointegration factor (BAF) compete for binding to emerin in vitro. J Biol Chem. 2003;278:6969–75. https://doi.org/10.1074/jbc.M208811200.

103. Gesson K, Rescheneder P, Skoruppa MP, von Haeseler A, Dechat T, Foisner R. A-type lamins bind both hetero- and euchromatin, the latter being regulated by lamina-associated polypeptide 2 alpha. Genome Res. 2016;26:462–73. https://doi.org/10.1101/gr.196220.115.

104. Harr JC, Luperchio TR, Wong X, Cohen E, Wheelan SJ, Reddy KL. Directed targeting of chromatin to the nuclear lamina is mediated by chromatin state and A-type lamins. J Cell Biol. 2015;208:33–52. https://doi.org/10.1083/jcb.201405110.

105. Solovei I, Wang AS, Thanisch K, Schmidt CS, Krebs S, Zwerger M, et al. LBR and Lamin a/C sequentially tether peripheral heterochromatin and inversely regulate differentiation. Cell. 2013;152:584–98. https://doi.org/10.1016/j.cell.2013.01.009.

106. Gruenbaum Y, Medalia O. Lamins: the structure and protein complexes. Curr Opin Cell Biol. 2015;32:7–12. https://doi.org/10.1016/j.ceb.2014.09.009.

107. Kochin V, Shimi T, Torvaldson E, Adam SA, Goldman A, Pack C-G, et al. Interphase phosphorylation of lamin A. J Cell Sci. 2014;127(Pt 12):2683–96. https://doi.org/10.1242/jcs.141820.

108. Barton LJ, Soshnev AA, Geyer PK. Networking in the nucleus: a spotlight on LEM-domain proteins. Curr Opin Cell Biol. 2015;34:1–8. https://doi.org/10.1016/j.ceb.2015.03.005.

109. Dechat T, Adam SA, Taimen P, Shimi T, Goldman RD. Nuclear lamins. Cold Spring Harb Perspect Biol. 2010;2:a000547. https://doi.org/10.1101/cshperspect.a000547.

110. Bronshtein I, Kepten E, Kanter I, Berezin S, Lindner M, Redwood AB, et al. Loss of Lamin a function increases chromatin dynamics in the nuclear interior. Nat Commun. 2015;6:8044. https://doi.org/10.1038/ncomms9044.

111. Bank EM, Gruenbaum Y. The nuclear lamina and heterochromatin: a complex relationship. Biochem Soc Trans. 2011;39:1705–9. https://doi.org/10.1042/BST20110603.

112. Politz JCR, Scalzo D, Groudine M. Something silent this way forms: the functional organization of the repressive nuclear compartment. Annu Rev Cell Dev Biol. 2013;29:241–70. https://doi.org/10.1146/annurev-cellbio-101512-122317.

113. Zheng X, Kim Y, Zheng Y. Identification of Lamin B-regulated chromatin regions based on chromatin landscapes. Mol Biol Cell. 2015;26:2685–97. https://doi.org/10.1091/mbc.E15-04-0210.

114. Hofmann WA, Johnson T, Klapczynski M, Fan J-L, de Lanerolle P. From transcription to transport: emerging roles for nuclear myosin I. Biochem Cell Biol. 2006;84:418–26. https://doi.org/10.1139/o06-069.

115. Ondrej V, Lukásová E, Krejčí J, Matula P, Kozubek S. Lamin a/C and polymeric actin in genome organization. Mol Cells. 2008;26:356–61.

116. Spichal M, Brion A, Herbert S, Cournac A, Marbouty M, Zimmer C, et al. Evidence for a dual role of actin in regulating chromosome organization and dynamics in yeast. J Cell Sci. 2016;129:681–92. https://doi.org/10.1242/jcs.175745.

117. Kind J, Pagie L, Ortabozkoyun H, Boyle S, de Vries SS, Janssen H, et al. Single-cell dynamics of genome-nuclear lamina interactions. Cell. 2013;153:178–92. https://doi.org/10.1016/j.cell.2013.02.028.

118. Dixon JR, Selvaraj S, Yue F, Kim A, Li Y, Shen Y, et al. Topological domains in mammalian genomes identified by analysis of chromatin interactions. Nature. 2012;485:376–80. https://doi.org/10.1038/nature11082.

119. Live Cell Imaging: A laboratory manual. Cold Spring Harbor laboratory press; 2004.

120. Nabbi A, Riabowol K. Rapid isolation of nuclei from cells in vitro. Cold Spring Harb Protoc. 2015;2015:769–72. https://doi.org/10.1101/pdb.prot083733.

121. Villalobos DP, Bautista R, Cánovas FM, et al. Isolation of bacterial artificial chromosome DNA by means of improved alkaline lysis and double potassium acetate precipitation. Plant Mol Biol Rep. 2004;22:419 doi.org/10.1007/BF02772684.